Chemical Engineering Journal 452 (2023) 139202

Contents lists available at ScienceDirect

Chemical Engineering Journal

journal homepage: www.elsevier.com/locate/cej

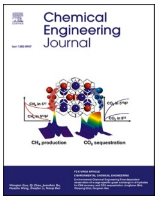

A recent overview of per- and polyfluoroalkyl substances (PFAS) removal by functional framework materials

Huarui Li [a,b], Allyson L. Junker [a], Junying Wen [a], Lutz Ahrens [c], Mika Sillanpää [a], Jiayu Tian [d], Fuyi Cui [e], Leendert Vergeynst [a], Zongsu Wei [a,*]

[a] Centre for Water Technology (WATEC) & Department of Biological and Chemical Engineering, Aarhus University, Universitetsbyen 36, 8000 Aarhus C, Denmark
[b] School of Civil Engineering, Yantai University, Yantai 264005, PR China
[c] Department of Aquatic Sciences and Assessment, Swedish University of Agricultural Sciences (SLU), Box 7050, SE-750 07 Uppsala, Sweden
[d] School of Civil Engineering and Transportation, Hebei University of Technology, Tianjin 300401, PR China
[e] College of Environment and Ecology, Chongqing University, Chongqing 400044, PR China

ARTICLE INFO

Keywords:
Per- and polyfluoroalkyl substances (PFAS)
Framework materials
Zeolites
Metal-organic frameworks
Covalent organic frameworks

ABSTRACT

Per- and polyfluoroalkyl substances (PFAS) are a class of toxic and bioaccumulative compounds affecting environmental and human health. Conventional wastewater treatment processes are ineffective at remediating these persistent chemicals. While functional framework materials have been shown to remove PFAS via adsorption and catalytic degradation, there is an on-going debate about their practical use in water purification. Inspired by recent research on typical functional framework materials, including zeolites, metal-organic frameworks (MOFs), and covalent organic frameworks (COFs), our review summarizes the principles of their design, properties, and applications with a special emphasis on PFAS removal. The potential of framework material for catalytic degradation of PFAS is constructively discussed, based on limited studies thus far. Finally, the challenges of using framework materials to remove and degrade PFAS in wastewater are presented along with sustainable design prospects to improve the technology. The current review provides new insights in advancing framework materials for PFAS elimination from contaminated waters.

1. Introduction

1.1. Background

1.1.1. Per- and polyfluoroalkyl substances

Per- and polyfluoroalkyl substances (PFAS) are a group of anthropogenic compounds comprising over 6,500 individual chemicals [1]. The fluorine atoms stiffen the alkyl chain by forming characteristic structures called “molecular brush” on the PFAS molecules, yielding its unique properties [1,2]. PFAS have extreme biological, chemical and physical stability due to the carbon–fluorine bond, leading to high potential of bioaccumulation [3,4]. PFAS have been broadly utilized in many industrial and commercial applications (e.g., textile, repellents, food packaging, shampoos, cookware, cleaners, polishers, and aqueous firefighting foams) [5,6]. The majority of production and use (80%) has been released to the environment [7], making PFAS contaminants of high concern. While 2,610–21,400 tonnes of C4–C14 perfluoroalkyl carboxylic acids (PFCAs) have been emitted from 1951 to 2015, excessive emission of 20–6,420 tonnes has been projected between 2016 and 2030 [8]. By now, a large variety of PFAS have been detected globally, even in remote Arctic regions [9], with concentrations ranging from pg/L to μg/L levels [10]. In the United States, the number of PFAS-contaminated sites, including drinking water systems, has reached 620 across 43 different states [1]. It has been discovered that the effluent concentrations from 3M company’s “test locations” were about 586 ±243 ng/L for perfluorooctane sulfonate (PFOS) and 298 ±284 ng/L for perfluorooctanoate (PFOA) [11]. In another study [12], 32 PFAS were detected in a landfill leachate sample with 8300 ng/L perfluorohexanoic acid (PFHxA), 6500 ng/L perfluoroheptanoic acid (PFHpA), and 4800 ng/L PFOA among the highest. The concentration of these PFAS will be diluted to a much lower levels when entering the wastewater treatment plants (WWTPs), making wastewater effluents and biosolids perennial sources of PFAS contamination. Kunacheva et al. [13] analyzed surface water samples from 41 cities in 15 countries and revealed the occurrence of PFOS and PFOA in all samples, which ranged from non-detect to 70.1 ng/L and 0.2–1630.2 ng/L, respectively.

---

* Corresponding author.
E-mail address: zwei@bce.au.dk (Z. Wei).

https://doi.org/10.1016/j.cej.2022.139202

Human exposure to the PFAS can occur mainly through: 1) intake of food contaminated during farming or from food packaging and cookware [14]; 2) consumption of contaminated drinking water [15]; and 3) inhalation of dust and air containing PFAS [16]. Studies have illustrated that, in terms of PFOS and PFOA, food intake is probably the main exposure pathway [17]. Because of their persistence, PFAS can accumulate in biota over a long time [18], e.g., the half-life of PFOA and PFOS in human blood serum is approximately 3.5 and 4.8 years, respectively [19]. Epidemiological studies have linked specific PFAS to different adverse health effects, including reproductive and developmental effects, hepatic and metabolic toxicity, immunotoxicity, tumor induction, endocrine disruption, neurotoxicity, and obesity [20].

Due to these environmental and health concerns, the production and use of PFOA and PFOS are prohibited by the Stockholm Convention on Persistent Organic Pollutants. These regulations led to a change of production from long-chain PFAS to short-chain PFAS, which has been conducted by major manufacturers since the early 2000s. Several short-chain PFAS such as perfluorobutanoate (PFBA), perfluorobutane sulfonate (PFBS), and hexafluoropropylene oxide dimer acid (Gen X) are produced as substitutes for typical PFOA and PFOS [21]. Therefore, these shorter-chain analogues are widely detected in the environment. In addition, the long-chain PFAS precursors can generate short-chain PFAS through their environmental degradation [2]. These short-chain PFAS are more persistent, less adsorbable, and more mobile in soil and groundwater, leading to longer-distance transport and a wider range of adverse environmental impacts for decades to come [22]. However, the relationship between eco-toxicity and carbon chain length remains unclear [23]. Although some studies reported lower bioaccumulation potential, short-chain PFAS still showed enrichment properties in edible plants, while its accumulation in the food chain remains unknown [24]. So far, regulations for short-chain PFAS are still nascent.

Given the high exposure risk of PFAS, many water treatment technologies have been developed to remove them [22]. The conventional activated sludge treatment processes [25] or membrane bioreactor treatments [26] are ineffective in treating PFAS, since the mass flow of PFOA/PFOS stay the same or even increase in the effluent. Percursor compounds in the influent appear to undergo biodegradation during activated sludge treatment, thus, becoming a source of additional PFOA/PFOS in the secondary effluent [27]. Therefore, tertiary treatment is required for PFAS removal, e.g., adsorption, advanced oxidation/reduction, ion-exchange, membrane filtration, or sonolysis [25]. Despite some success, these treatment technologies are criticized for either high energy consumption or generation of pollutant-laden waste. Although photocatalytic degradation is a technique with low-energy consumption and mild operating conditions [25,28–30], it relies on the surface interactions with contaminants and is determined by the activity, selectivity, and stability of the catalyst [31]. Further research is therefore required to defluorinate PFAS sustainably and economically.

Several reviews have described materials for efficient PFAS removal from aqueous environment. Ateia et al. [32] provided a summary of amine-functionalized sorbents. Zhang et al. [33] summarized the current adsorbent materials and their adsorption isotherms, kinetics, and mechanisms. However, the role of framework materials to concentrate (as adsorbents) and then destroy PFAS (as active catalysts) has not been systemically reviewed yet. Framework materials have extraordinary adsorption capacities and selective reactivities. Hence, they merit researchers' attention when seeking effective methods for the removal and degradation of PFAS.

1.1.2. *Framework materials*

Framework materials are tailored, crystalline, and well-defined periodic structures. Their physiochemical properties are closely correlated with their chemical composition as well as structural and geometrical features. This review includes zeolite, metal–organic frameworks (MOFs), and covalent organic frameworks (COFs) in the category of "framework materials".

In 1756, Axel Cronstedt from Sweden first described zeolites, using the Greek *zeo* (boil) and *lithos* (stone) [40,41]. Currently, there are more than 200 known zeolite structures, including $[SiO_4]^-_4$ and $[AlO_4]^-_5$ tetrahedron. Zeolite held the record of the most porous material until the end of 20th century, when researchers proved that MOF-5 has three times higher internal surface area than most porous zeolite [42]. MOFs consists of a combination of organic and inorganic molecules which are connected by strong bonds; the strength of these linkages and the composition of the metal containing entity can be controlled. Researchers have created more than 20,000 MOFs [43].

In 2005, Yaghi's group demonstrated the principle for the preparations of organic frameworks bridged by covalent bonds, considered to be the first example of COFs synthesis [44]. Unlike MOFs, low-density COFs exhibited superior stability in various and extreme conditions [45], which is attributed to the strong covalent bonds in their framework structures. The higher porosity of COFs allows boosted diffusion, adsorption, and desorption of compounds.

In the last few decades, the framework materials have gained widespread use in gas storage [34], separation [35], absorption [36], catalysis [37], sensing, and as substrates for mechanistic studies [38,39]. The abundant active sites coupled with controllable pore structure, surface charge, and functional groups of framework materials are huge advantages toward selective PFAS adsorption. Moreover, framework materials have achieved excellent performance for PFAS catalytic degradation in several advanced oxidation systems [46,47]. Thus, framework materials, acting as both adsorbents and catalysts, have a high potential for removing PFAS from aquatic environment, validating the effort to seek new insights into these tunable materials.

1.2. *Scope of the review*

Given their large specific surface area, porous structure, tunable physiochemical properties and functionalities, framework materials are recognized for use in environmental remediation. Our review presents a comprehensive picture of the principles for framework materials such as zeolites, MOFs, and COFs for their superior removal of PFAS. All references were searched from mainstream sci-tech journal databases. We examined multiple studies on PFAS source, occurrence, effects, and especially removal by framework materials. However, research in this field is still in its early stage, with most literature focusing on adsorptive removal. Our discussion includes fundamental knowledge, and highlights of important results from 24 references over the last 14 years related to framework materials. Target PFAS chemicals are limited to PFOA, PFOS, Gen-X, etc. in this review, simply due to the early-stage research. Following this introduction in Section 1, Sections 2, 3, and 4 discuss the unique structure and synthesis of zeolite, MOFs, and COFs, respectively, as summarized in Table 1. The details of their synthesis methods are presented in the supplementary materials. Each section also presents of the adsorption and degradation mechanisms involved for PFAS removal. Section 5 is devoted to the impacts of initial concentration, solution pH, coexisting ions, and dissolved organic matter (DOM) on PFAS removal. Current and future research challenges are discussed in the last section.

The objective of the current review is to critically assess the feasibility of using framework materials to remove PFAS. It provides a road map to understand the current research status and fundamental principles of the adsorption and degradation processes. The PFAS classification, occurrence, and treatment technologies, which have been the focus in previously published review papers [48–51], are explicitly excluded from this review.

Table 1
Summary of synthesis methods of framework materials.

Method	Sample	Precursors	Solvent	Conditions	Ref
Diffusion	ZIF-67	Co^{2+}, HmIm	H_2O/DMF	RT, 48 h	[61]
Hydro /solvo-thermal	Zeolite	Silica and alumina source, NaOH, organic template	H_2O	>100 °C	[62]
	MOF-5	Zn^{2+}, H_2BDC	DMF	120 °C, 24 h	[42]
	CF_3-COF	Tb, Tf	1,4-dioxane/ n-butanol	25 °C, 12 h	[63]
Microwave	Cr-MIL-101	Cr^{3+}, H_2BDC	H_2O/EtOH	600 W, 210 °C, 40 min	[64]
	TF-COF	2,3,5,6-tetrafluoro-4-pyridinecarbonitrile, 2,3,6,7,10,11-hexahydroxy triphenylene	4-dioxane/ triethylamine	70 °C, 30 min	[65]
Electrochemical	Al-MIL-53	Al^{3+}, H_2BDC	H_2O/DMF	Electrolyte: KCl, 90 °C, 10 mA	[66]
Mechanochemical	HKUST-1	Cu^{2+}, H_3BTC	No solvent	25 Hz, 15 min	[67]
Sonochemical	Mg-MOF-74	Mg^{2+}, H_4DHTP	DMF/EtOH/H_2O	500 W, 1 h	[68]

HmIm: 2-Methyl imidazole; DMF: N,N-dimethylformamide; RT: Room temperature; H_2BDC: Terephthalic acid; EtOH: Ethanol; H_3BTC: Trimesic acid; H_4DHTP: 2,5-dihydroxybenzene carboxylic acid; Tb: 1,3,5-triformylbenzene; Tf: 3,3'-bis(trifluoromethyl)benzidine.

2. Zeolites

2.1. Structure of zeolites

Zeolites are hydrated aluminosilicates of alkali with porous and crystalline structure. Their frameworks are consisted of corner-shared $[SiO_4]^{4-}$ and $[AlO_4]^{5-}$ tetrahedrons connected by pore openings, forming different cage structures (Fig. 1). The pore sizes are determined by the structural type and usually range from 0.3 to 1 nm. It has been verified that the positively charged cations (univalent or bivalent metals) located within the pores neutralize the negative charge on the lattice [54]. According to the crystallographic unit cell zeolite structure, their structural formula can be written as: $M_{x/n}[(AlO_2)_x(SiO_2)_y]wH_2O$. Here, the (M) represents an alkaline cation, (n) represents its valence, x and y are tetrahedrons numbers in each unit, and (w) means the amount of water molecules. Normally, the ratio of y/x can range from 1 to 100 [40]. Moreover, transforming the topological structure of synthesized zeolites is another strategy, which has been applied in transforming two-dimension to three-dimension and three-dimension to three-dimension structures [55].

2.2. PFAS removal by zeolite

Owing to their porous structure and favorable chemical properties, zeolites can act as molecular sieves and catalysts for gas separation [56], adsorption process [57], and catalytic conversion of biomass [58]. Recently, zeolite and zeolite-based materials have attracted large attention for PFAS adsorption and catalytic degradation [46,47,59,60].

2.2.1. Adsorptive removal of PFAS

Three faujasites were chosen to evaluate their capacity for PFOS adsorption. Their Si/Al ratios varied from 2.8 (13X) to 80 (NaY80) [59]. As shown in Fig. 2a, the PFOS adsorbed to the NaY80 zeolite, but hardly adsorbed to the 13X and NaY zeolites (Si/Al = 5.5 for NaY). The high silica content endows NaY80 with most hydrophobic surface among these zeolites. Thus, hydrophobic interactions were inferred to dominate the adsorption process of PFOS.

Bergh et al. [60] proposed an all-silica beta type zeolite with strong hydrophobicity; it exhibited high efficiency and selectiveness for typical PFAS removal, *i.e.*, PFOA and PFOS. Fig. 2b displays its high adsorption capacities for PFOA and PFOS uptake, which is better than more widely used activated carbon (AC). The author proposed that the PFOA molecules are located in the *a*- and *b*-channels in zeolite inner structure, while the carboxylic heads interacted with hydrophobic chains to form a hydrogen bond (Fig. 2c), resulting in a very favorable adsorption enthalpy.

2.2.2. Advanced oxidative removal of PFAS

Qian et al. [46] utilized Fe-loaded zeolites (Fe-BEA35) as a PFOA sorbent, then combined it with photochemical defluorination. Under

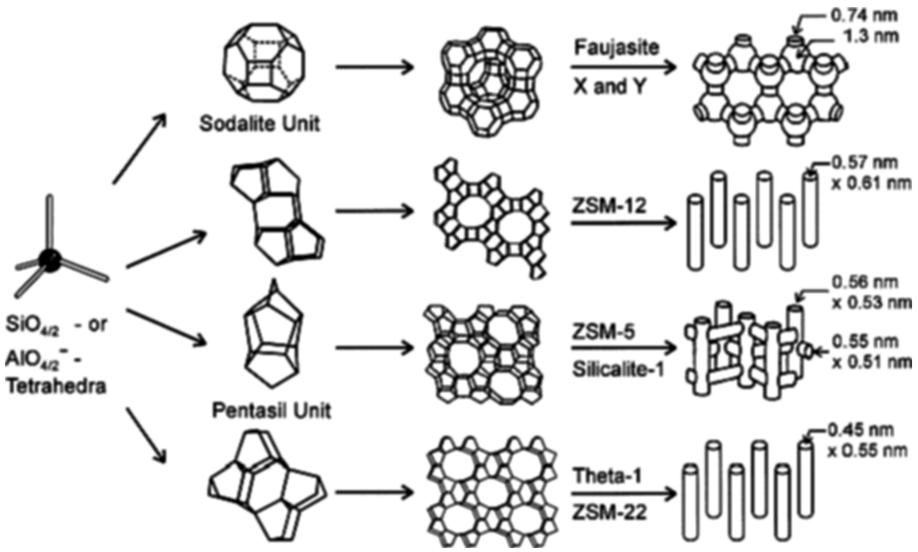

Fig. 1. Structure of secondary building units (SBUs), zeolite frameworks and their micropore systems and dimensions. Replotted from ref [52,53]. Copyright 2000 Elsevier.

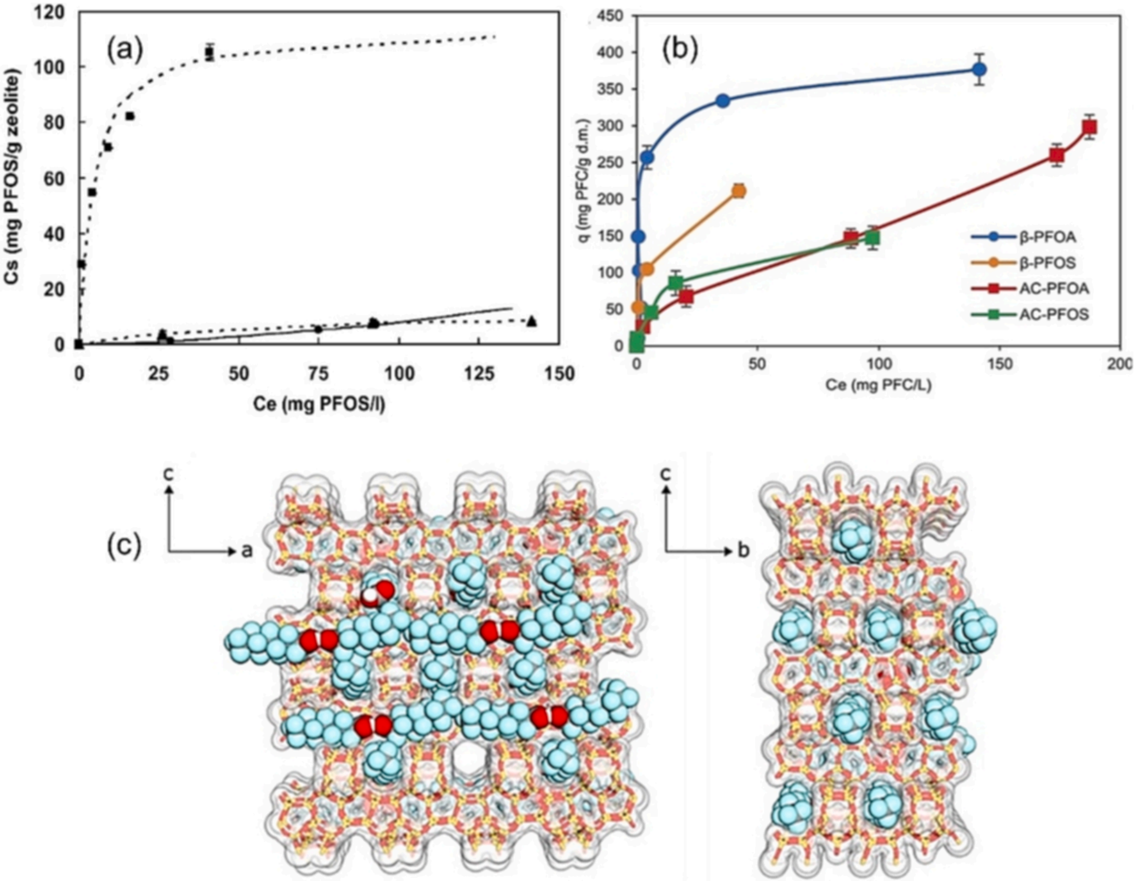

Fig. 2. (a) Adsorption isotherms of PFOS on NaY80 (■), NaY (●), and 13X (▲) (Replotted from ref [59]. Copyright 2008 Elsevier). (b) PFOA and PFOS adsorption isotherms (293 K) on all-silica Beta (β) and activated carbon (AC). (c) Diagrammatic sketch of all-silica zeolite Beta adsorbing PFOA molecules. Replotted from ref [60]. Copyright 2020 Wiley.

UV-A irradiation, the Fe-zeolite efficiently degraded the adsorbed PFOA (i.e., 99 % removal in 24 h, pH = 5.5) (Fig. 3a). The Fe-BEA35 showed different catalytic performance under oxygen and nitrogen conditions and the defluorination efficiency was detected to be 22 % and 2.1 %, respectively. These results indicated the contribution of molecular oxygen as the source of reactive species that promote the oxidation and mineralization of PFOA intermediates. Molecular oxygen is a direct participant in the radical chemistry of PFOA decomposition. It also served as the oxidizing agent in the ferrous iron's re-oxidation to ferric iron.

As depicted in Fig. 3b, the ferric ions on zeolite complexed with PFOA and adsorbed it non-specifically. As a result, the carboxylic group is close to Fe^{3+}, making it possible for the charge to transfer from carboxylate to metal under irradiation. At the same time, the charge transfer is unlikely for the non-specifically adsorbed PFOA. Hence, the defluorination pathway often occurs with the decarboxylation as the first step yielding perfluorinated alkyl radicals ($C_8F_{17}\bullet$). Then, the formed $C_8F_{17}\bullet$ can combine with either H_2O, OH^-, or hydroxyl radicals ($^\bullet OH$) to yield unstable perfluorinated alcohol, $C_8F_{17}OH$, that undergoes stepwise elimination of $-CF_2$ groups, until completely defluorinated.

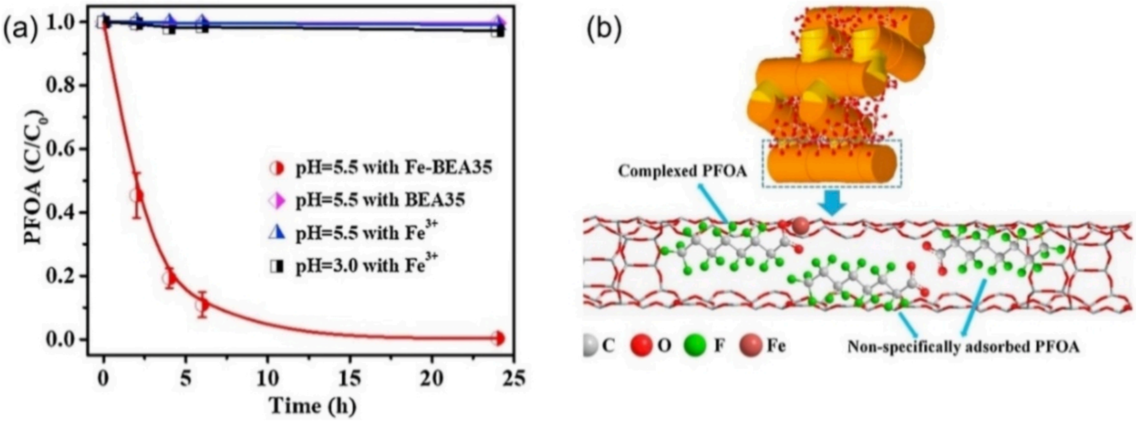

Fig. 3. (a) PFOA degradation under UV-A irradiation. (b) Different configurations of PFOA adsorbed onto the zeolite. Replotted from Ref [40]. Copyright 2020 Elsevier.

Fig. 4 presents the proposed defluorination pathways for perfluoroalkyl carboxylic acids (PFCA) and perfluoroalkyl sulfonates (PFSA) by radical-based reactions.

Prior to degradation, the key step is adsorption, influenced by the electrostatic attractions between negative $R-COO-$ and positive Fe^{3+} along with the hydrophobic effect of perfluoroalkyl tail of $R-$[46,59]. When the hydrophobic interactions dominate the PFAS adsorption process, PFAS with longer chain lengths was more readily adsorbed, due to their higher hydrophobicity [69]. Accordingly, the adsorbed fraction of perfluoroalkyl carboxylates (PFCAs) decreased with decreasing chain lengths. Thus, it is demonstrated that hydrophobic effect dominates the PFCA adsorption on Fe-zeolites.

Furthermore, it was reported that the microscale Fe-BEA35 can degrade PFOS under UV-C irradiation (Fig. 5a) [47]. When quantifying PFOS desulfurization ratio in UV/persulfate system, the quantification of sulfate ions should be carefully carried out to exclude the interference of persulfate-converted sulfate ions. PFOS adsorption onto Fe-BEA35 occurred both nonspecifically and complexed at ferric ions, as shown in Fig. 5b. Under UV irradiation, the complex, $C_8F_{17}SO_3$-Fe, was excited to produce $C_8F_{17}SO_3^{\bullet}$ that desulfurized to $C_8F_{17}^{\bullet}$. Further decomposition involving H_2O, OH^-, or $^{\bullet}OH$ followed the same pathway as PFOA defluorination (as presented in Fig. 4). The effective mineralization of PFOS and its intermediates was realized by regenerating the catalyst via UV irradiation with the addition of sodium persulfate. Although the residual PFOS and byproducts extracted from zeolite were analyzed, the fluoride ion adsorption on zeolite is also recommended as a control test to properly measure fluoride ions when determining defluorination rates. The PFOS degradation in the contaminated groundwater was as efficient as that in the synthetic solution, establishing the potential of this photochemical process in real water matrices.

These examples provide new insights into the interactions between iron species and PFAS and the degradation mechanisms involved. Further efforts are needed to develop other zeolite-based materials and improve photocatalytic defluorination rates. Meanwhile, it is important to figure out the defluorination chemistry of PFAS complexed on Fe-zeolites, including the evolution of reactive species and degradation pathways.

3. Metal organic frameworks (MOFs)

3.1. Structure of MOFs

MOFs are a class of crystalline, porous functional materials comprised of metal ions and organic linkers. The positively charged metal ions act as nodes that connect with the linkers to build a periodic structure. The different combination of metal species and organic linkers modulates the crystalline structure and physiochemical properties. The various metal centers have different coordination modes: Divalent transition metals ions (e.g., Zn(II), Cu(II), Cd(II), and Co(II)) tend to adopt an octahedral, six-coordination mode, while the rare earth metals (e.g., Ln(III)) generally have an eight or nine-coordination mode [70]. Meanwhile, the coordination groups and geometric shapes of different organic ligands also vary. Linear carboxylic acid ligands (e.g., terephthalic acid) tend to bridge metals or metal clusters in a straight line, whereas V-shaped carboxylic acid ligands (e.g., 1,3,5-benzene tricarboxylate) tend to form a cage-like, porous structure with the metal nodes [71–73]. Herein, some typical Secondary Building Units (SBU) of MOFs structures are described.

(1) $Zn_4O(O_2CR)_6$

In the year of 1999, Yaghi's group first synthesized the well-known MOF-5 ($ZnO_4(BDC)_3(DMF)_8C_6H_5Cl$) with a three-dimensional porous structure (Fig. 6a) [42]. The SBU of MOF-5 is the octahedral configuration of $Zn_4O(O_2CR)_6$. Its Langmuir specific surface area and pore volume reached 2900 m^2/g and 0.61 cm^3/g, respectively. Its thermal stability reaches 400 °C. Building upon MOF-5, Yaghi's team prepared a group of isoreticular MOFs (IRMOFs) with different pore sizes through functional group modification of the bridged terephthalic acid and extension of the linear ligand length. As a result, they obtained MOFs with ideal pore size for high capacity methane storage [88].

(2) $Cu_2(O_2CR)_4$

The copper, paddlewheel shaped unit is coordinated equatorially by four ligand carboxylates. When combined with trimesic acid, another famous MOF structure was formed: HKUST-1 (Fig. 6b) [89], which has a neutral skeleton with high Langmuir surface area (917.6 m^2/g) and porous structure (0.61 cm^3/g). When thermal activation and other methods are used to remove solvent molecules, the binuclear metal copper ion forms an open metal site, which acts as a functional site for gas adsorption. Through lengthening the prototype ligands or swapping the tricarboxylic acid for hexacarboxylic or octacarboxylic acid, researchers prepared a series of derivative structures with larger specific surface areas and pore sizes [90–92].

(3) Zeolite Imidazolate Framework (ZIF)

Yaghi's group prepared a series of ZIF crystals by reacting Zn(II) ions with nitrogen-containing heterocyclic imidazole or purine ligands (Fig. 6c) [93]. The crystal structure is characterized by four-coordination metal ions and a 145° bond angle of *T*-Im-T (Im = imidazolate, T = tetrahedrally coordinated metal ion), which is close to the Si-O-Si bond angle in zeolite $(Al)SiO_2$. Therefore, the crystal structure of ZIF shares the sodalite topological structure with zeolite. Likewise, the chemical and thermal stability of ZIF is similar to zeolite crystals, i.e., the thermal stability up to 600 °C.

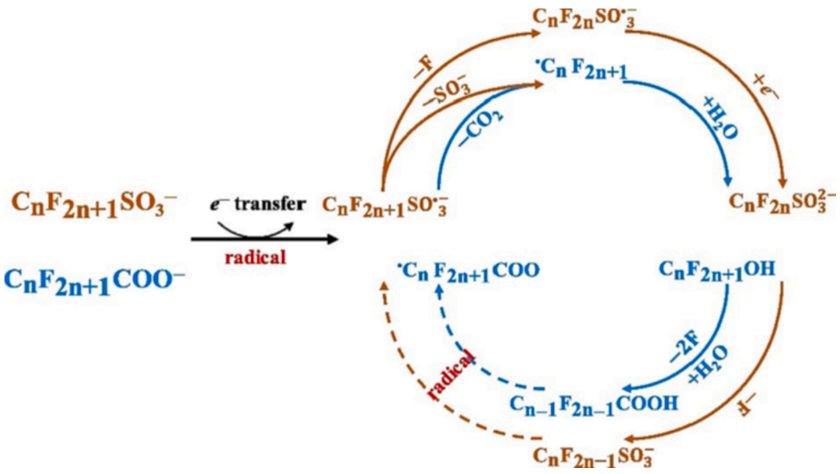

Fig. 4. Radical-based reactions induced PFCAs and PFSAs defluorination. Replotted from Ref [5]. Copyright 2020 Elsevier.

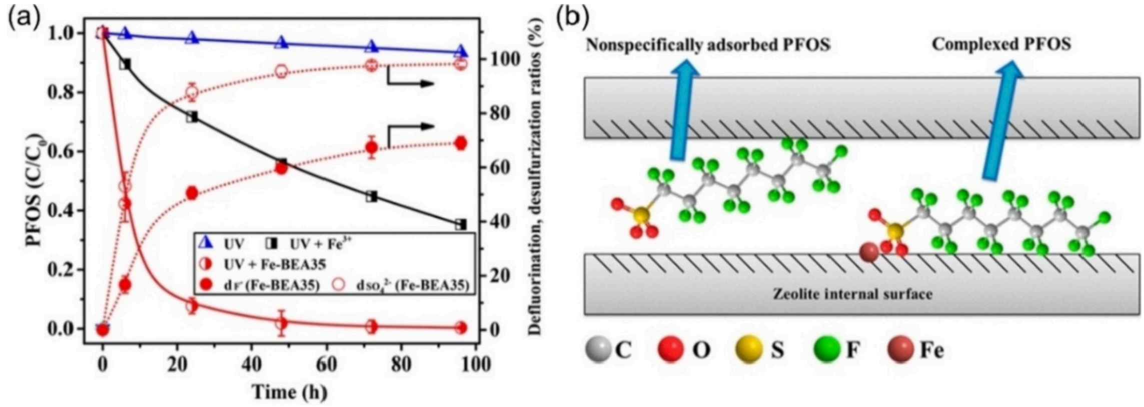

Fig. 5. (a) PFOS degradation and intermediates formation. (b) Two types of PFOS adsorption on Fe-BEA35. Replotted from Ref [47]. Copyright 2021 American Chemical Society.

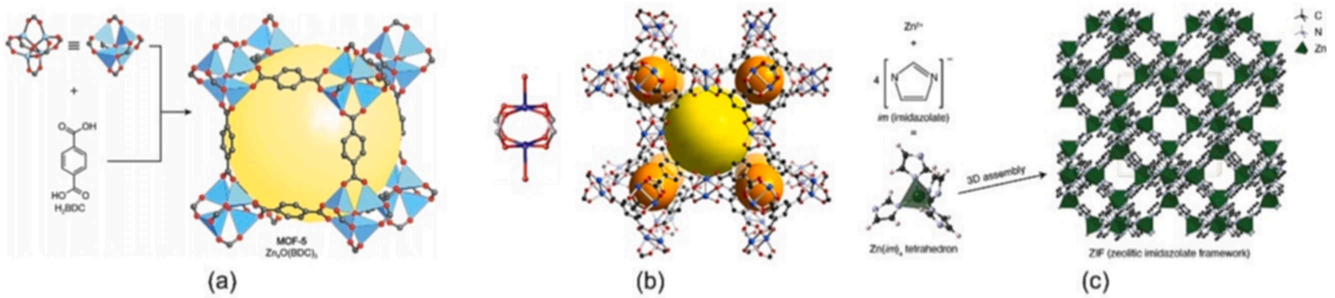

Fig. 6. (a) $Zn_4O(O_2CR)_6$ and MOF-5 structure (Replotted from ref [87]. Copyright 2019 Wiley). (b) $Cu_2(O_2CR)_4$ and HKUST-1 structure. (c) Zeolite Imidazolate Framework (ZIF) structure. Replotted from Wikimedia Copyright Creative Commons.

3.2. PFAS removal by MOFs

3.2.1. Adsorptive removal of PFAS

(1) Pristine MOFs

Several kinds of MOFs have been reported to effectively remove PFAS from polluted water. One example is MIL-101(Cr), a chromium (III) terephthalate MOF, which has high stability, acid-base resistance, and large specific surface area ($S_{BET}\approx4000$ m^2/g). The target organic substrate can enter its quasi-spherical cages, resulting in good PFAS removal [94]. An Al-based MOF (MIL-53) was also synthesized for PFOA adsorption, as well as two other organic contaminants (bisphenol A (BPA) and 17α-ethynylestradiol (EE2)). The MIL-53 reached its highest adsorption capacities of 138, 200, and 169 mg/g for BPA, EE2, and PFOA, respectively [82].

As an abundant and non-toxic metal species, iron-based materials have been widely utilized in environmental remediation. Iron-based MOFs have been investigated to remove PFAS. Yang et al. [81] demonstrated higher PFOA adsorption capacity of Fe-BTC compared to MIL-100-Fe and MIL-101-Fe. Multiple adsorption mechanisms of PFOA on Fe-based MOFs have been proposed, including Lewis acid/base (LAB) interaction, π-CF attraction, anion-π interaction, and hydrogen bond. LAB complexing played a dominant role due to its higher binding energy. Li et al. [76] found that the mesoporous cationic thorium-organic framework (SCU-8) can immobilize PFOS anions through electrostatic attraction, hydrophobic interaction, hydrogen bond, and van der Waals force at different step.

Preliminary research on the impact of metal species on removing PFAS have been investigated. Barpaga et al. [78] utilized chromium and iron analogs of MIL-101 to investigate the sorption of PFOS. XPS analysis revealed stronger interactions between metal nodes and PFOS's sulfur moieties, indicating Cr-MIL-101′s higher efficiency for PFOS removal. Zhao et al. [95] recently compared MIL-53(Al), MIL-53(Fe) and MIL-101 (Cr) and demonstrated that MIL-53(Al) exhibits the highest PFOS adsorption capacity, because it has more unsaturated metal sites and a smaller pore size. For a typical PFAS substrate and MOF structure, metal species play an important role in removing PFAS, since different metal nodes exhibited different interaction capacity.

In addition to the metal species, the organic linker, crystal structure and other surface properties determine the PFAS removal capacity of MOFs. Chen et al. [75] inspected how the topological structure and interior functionality affect PFOA removal. ZIF-7 and ZIF-8 have same topology, but are made up of different ligands. Similarly, ZIF-8 and ZIF-L are both comprised of zinc ion, but the organic ligands have different crystal structures. Compared to ZIF-7, ZIF-8 exhibited better performance toward PFOA sorption, suggesting the interaction between 2-methylimidazole and PFOA are stronger [75]. ZIF-L outperformed other tested sorbents for PFOA removal due to its layered structure, implying that PFOA diffusion into the interlayer proceeds with less resistance than into cylindrical micropores.

(2) Modified MOFs

It has been proven that surface modification can improve MOFs adsorption capacity toward PFAS. Partially hydrolyzed poly-acrylamide (HPAM) assisted modification affected the particle size and crystal morphology of MIL-96. Added amine surface functionality enhanced the PFOA removal efficiency by increasing the electrostatic interaction between positively-charged amine and PFOA anions [83]. A comparison of PFAS removal by pristine UiO-66 versus its equivalent perfluorinated MOF, UiO-66-(F4), revealed that UiO-66-(F4) is more efficient due to increased van der Waals interactions between the fluorinated cavity of the MOF and fluorine on PFAS. Introducing defects into UiO-66 framework can increase the internal surface area and unsaturated Zr sites, leading to significant improvement of its adsorption capacity for PFOS and PFBS [77]. Liu et al. [74] studied a group of MIL-101(Cr)-based anion-exchange MOFs for PFOA adsorption and reported the highest adsorption capacity of 1.19 and 1.89 mmol/g for materials prepared by preassembled modification (PAM) and post-synthetic modification (PSM), respectively; the major adsorption mechanisms were LAB complexation and electrostatic interaction.

(3) MOFs based composites

By combining MOFs with nanomotor technology, Guo et al. [80] reported a buoyancy-propelled CAT-ZIF-8 nanomotor for simultaneous heavy metal and PFAS uptake. With the usage of hydrogen peroxide (0.2 %), the CAT-ZIF-8 exhibited controllable motion in the contaminated water, thus, significantly enhancing its removal efficiency.

To immobilize adsorptive frameworks, Moreton et al. [96] prepared a mixed-matrix membrane (MMM) from UiO-66 and poly(ethylene-*co*-vinyl acetate) and tested its performance for filtration and sorption of a 500 mg/L PFOA-solution. They successfully demonstrated PFOA removal using a hybrid membrane in dead-end filtration mode.

However, the adsorptive removal of PFAS cannot solve the problem fundamentally since it only transfers the pollutants from aqueous phase onto the solid phase. Subsequent extraction and degradation of PFAS adsorbed onto MOFs must be carried out to eliminate any PFAS pollution.

3.2.2. Advanced oxidative removal of PFAS

AOPs catalyzed by MOFs and MOF-based materials are a promising remediation strategy for degrading and mineralizing emerging contaminants, including PFAS. Hydro-stability is a crucial requirement for materials utilized in water treatment processes, especially in catalytic degradation processes. Ozdemir et al. [84] developed a chemically stable MOF (MIL-125-NH_2) from high valent Ti^{4+} clusters as building units. MIL-125-NH_2 was stable in different pH condition and adsorbed PFOA and PFOS efficiently (42 and 17 mg/g, respectively). Subsequent degradation of adsorbed PFOS was achieved through a reduction reaction under UV irradiation, where triethanolamine (TEOA) was the sacrificial reductant. TEOA transfered an electron to PFOA/PFOS to initiate the stepwise elimination of -CF_2, as demonstrated in Fig. 4. The Ti-MOFs demonstrated the combined superiority of both excellent PFAS adsorptive removal and photocatalytic reduction performance.

Although only a few works have reported PFAS degradation by MOF-catalyzed reactions, some pristine MOFs have showed excellent performance in catalytic degradation of other persistent organic pollutants [97,98]. There are also several strategies to further enhance their catalytic activity, such as functionalization of metal-clusters or ligands. For instance, Pu et al. [99] synthesized MIL-53(Fe) with high content of Fe^{2+} at coordinatively unsaturated sites (CUS), which exhibited high efficiency for activating persulfate. Goh et al. [100] demonstrated that using NH_2-BDC and F-BDC as mixed linkers to prepare Zr-MOF can enhance its photocatalytic activity.

On the other hand, combining MOFs to form heterostructures is an effective solution to overcome their individual disadvantages. Combining MOFs and graphitic carbon nitride (g-C_3N_4) can accelerate the photo-generated charge separation and increase the light absorption range, leading to better photocatalytic performance [101]. Likewise, coupling CdS with MOFs is a smart method to prevent particle aggregation, electron-hole pair recombination, and inhibition due to photocorrosion. Shen et al. [102] synthesized CdS-UiO–66(NH_2) nanocomposites through a facile photodeposition method. The synthesized materials showed excellent photocatalytic activity due to their large specific surface area and the efficient charge transfer from CdS to UiO–66(NH_2).

Developing similar MOF-based materials for PFAS removal and degradation is feasible but requires more attention. While MOFs can efficiently adsorb PFAS from aquatic environment, more efforts are needed to improve the catalytic oxidation capacity of MOFs for PFAS degradation.

4. Covalent organic frameworks (COFs)

4.1. Structure of COFs

Similar to MOFs, COFs are crystalline, porous, and organic structures whose atoms are linked by covalent bonds. Kandambeth et al. [103] summarized the reactions and symmetric combinations used for COF construction (Fig. S2). The COF crystallinity depends on the proper design of the organic building blocks [104]. Reversible bond formation, which imparts error-correction by itself during the crystallization, is essential [103]. Previously, the formation of reversible covalent bond was only observed at extreme conditions e.g., high temperature and pressure [103]. In 2013, Beaudoin et al. [105] first reported the formation of covalent bond with low strength under ambient conditions, resulting in monocrystalline network solids. To maintain the reversibility, a specific chemical agent was added in this process.

Researchers have successfully employed several reversible condensation reactions, including Schiff base reaction, Spirobrate formation, Knoevenagel condensation, and Imide condensation, for the crystallization of COFs [103]. Fig. S2 displays different kinds of reversible organic reactions and symmetry combinations applied for COF crystallization [103]. Using rigid symmetric organic linkers, COFs were constructed with variable pore shapes and sizes, including hexagonal, square, triangular and rhombic pore configurations (Fig. S2c). Moreover, reticular structures of COFs constructed by the linkage of various symmetric monomers resulted in their unique structures. Although they are vulnerable in aqueous environment, COFs have exhibited high stability and rigidity under thermal condition [103]. Moreover, COFs can be designed with different functional groups, e.g., imine groups [106]. COFs also possess a uniform nanopore network structure with high specific surface area. For example, 3D COF-103 has a reported S_{BET} of 4210 m^2/g [107,108]; its reported pore size ranges from 0.5 to 4.7 nm [109].

Given these unique features, COFs play important roles in adsorption, micro-extraction, sensor technology, and other applications [110]. COFs are a candidate for PFAS removal because of their tunable surface hydrophobicity, optional F-F affinity, adjustable functional groups, suitable pore shapes and sizes, and large specific surface area [32,63,108]. Positively charged functional groups, such as amine, attract the anionic part of ionized PFAS, while COFs' hydrophobic properties make interactions with the hydrophobic tail possible. Generally, the COFs have larger pore size than PFAS molecules, favoring its adsorption; when the pore size is tailored, selective capture of a specific PFAS is possible [86].

4.2. PFAS removal by COFs

4.2.1. Adsorptive removal of PFAS

The crystallinity of COFs enables them to have precise arrangements of functional groups with strong affinity for PFAS. There are four ways to improve COFs' adsorption capacity for PFAS: 1) Establish electrostatic interactions between functional groups; 2) add fluoro-functional groups to enhance F-F affinity; 3) increase hydrophobic interactions; and 4) achieve high specific surface area and establish the proper pore size for selective adsorption.

Positively charged COFs interact electrostatically with negatively charged PFAS. Wang et al. [86] compared the removal efficiency of neutral and cationic COFs, synthesized via solvothermal method (Fig. 7a), to remove GenX and hexafluoropropylene oxide trimer acid (HFPO-TA). Quaternary ammonium groups impart a positive charge to the novel cationic COF. Fig. 7b illustrates the higher adsorption capacity for Gen X and HFPO-TA by the cationic COF versus non–cationic COF. The cationic COF had a high adsorption capacity of HFPO-TA (2.16 mmol/g) and GenX (2.06 mmol/g) (Fig. 7c). It exhibited more than 92 % removal of HFPO-TA within 6 h and almost 100 % of HFPO-TA within 12 h (Fig. 7d). Ji et al. [85] also demonstrated that amine-functionalized

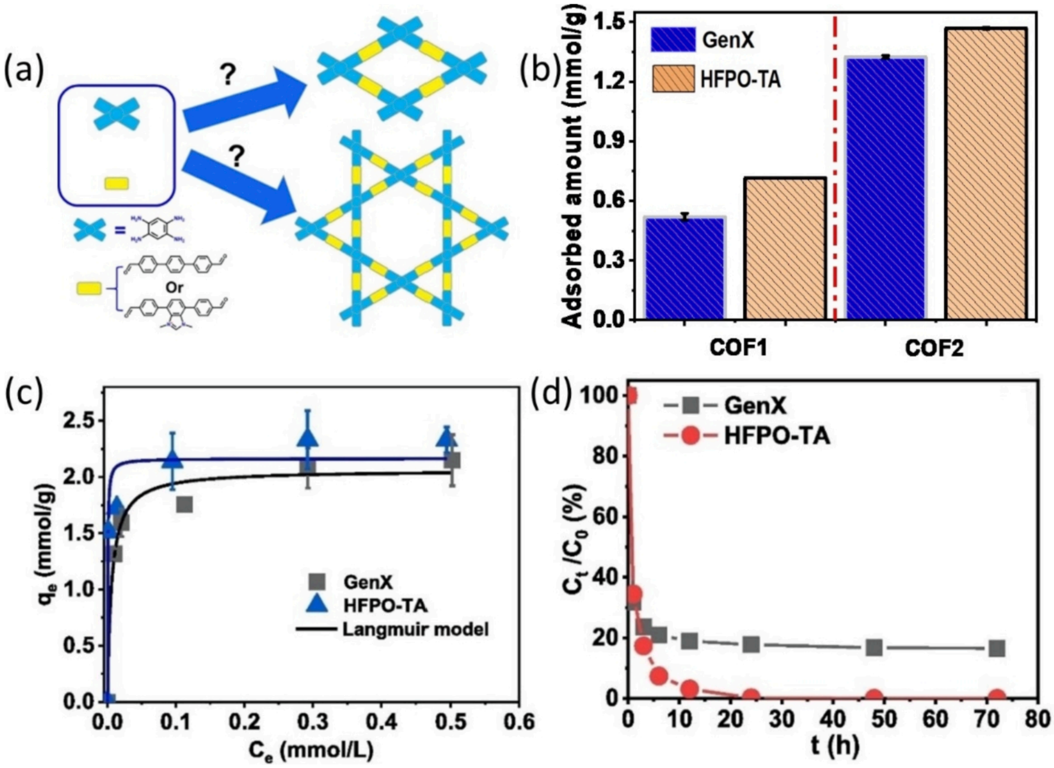

Fig. 7. (a) Synthesis scheme for neutral and cationic COFs; (b) The adsorption capacity of neutral COF1 and cationic COF2; (c) Langmuir adsorption isotherms of GenX and HFPO-TA on COF2; and (d) Removal of GenX and HFPO-TA by COF2. [86] Copyright 2021 Elsevier.

networks facilitate the interaction with anionic head groups of Gen X. Among all the prepared adsorbents, the amine-COF (28% by weight) had the highest affinity towards 13 PFAS. The removal efficiency was more than 90% for 12 out of 13 PFAS species, while the removal efficiency of Gen X was 91% after 30 min.

Fluoro-functionalized absorbents showed improved extraction performance for PFAS [63]. Sun et al. [63] synthesized a trifluoromethyl COF (CF_3-COF) by a sonochemical method at room temperature and used it as an epoxy resin coating for SPME. Eight targeted PFAS, including PFOA and PFOS, were eluted with 1 mL acetonitrile. This COF showed outstanding sensitivity to the targeted PFAS due to its fluorine affinity. The limits of detection for the solid phase micro-extraction (SPME) ranged from 0.1–0.7 pg/g to 0.2–0.8 pg/g for targeted PFAS.

Fluorine groups also play a dominant role in hydrophobic interactions between the PFAS tails and the COF's pore walls. In most cases, hydrophobic and electrostatic interactions have a combined effect in adsorbing PFAS. Adsorbents with amine groups have higher affinity for PFSA in comparison to PFCA with similar chain length, due to the higher hydrophobicity of PFSA [32]. In addition, long-chain PFAS are easier to be absorbed than shorter chain PFAS, which rely on electrostatic interactions [32]. Hou et al. [111] synthesized a superhydrophobic, fluoro-functionalized COF as a micro-extraction probe to adsorb 14 PFAS. This COF was synthesized by solvothermal method. The detection limit for the targetd PFAS varied from 0.02 to 0.8 ng/L in complex matrices (including water, urine, and milk). However, they did not quantify the contribution of F-F and hydrophobic interactions.

The high specific surface area of COFs provides more functional groups and active sites, and faster sorbate diffusion rates [32]. The specific surface area of TH-COF was as high as 1254 m^2/g, which substantially facilitated the diffusion of PFAS to the active sites [65]. When utilized as the coating for SPME, TH-COF provided extremely low detection limits of 0.0020–0.0045 ng/L in drinking, underground and river water samples. In addition, TH-COF was re-used 20 times without showing any decrease in extraction performance.

Proper pore size is another important determinant of adsorption capacity. Wang et al. [86] concluded that cationic COF with smaller pore size (about 1.4 nm) led to a steric effect while a larger pore size of 1.9 nm showed enhanced adsorption of HFPO-TA, which has a molecular size of 1.02 nm. This COF exhibited high capacity for absorbing GenX (2.06 mmol/g) and HFPO-TA (2.16 mmol/g), due to favorable pore structure and functional groups, i.e., quaternary ammonium groups.

4.2.2. *Advanced oxidative removal of PFAS*

While COFs have been widely used to catalyze hydrogen evolution [112,113] and carbon dioxide reduction [114], their semiconductor properties have also been considered for pollutant degradation [115]. Photoconductive COFs possess suitable energy band gap for the rapid diffusion of charge carriers within the framework [116]. Generally, the excited electrons in photoconductive COFs are transferred from donor to acceptor, thus facilitating electron-hole pair separation. For example, CTF-BT exhibited a broad adsorption band up to 550 nm [116].

In general, the building blocks of COFs are highly π-conjugated, which are fundamental in sheet stacking [117]. π-conjugated units are very important in harvesting light because the $\pi \rightarrow \pi^*$ transition occurs in the range of visible light (380–780 nm) [116]. Therefore, photoconductive COFs are sensitive to visible light with relatively small band gaps (~2.1–3 eV) [112,113,116]. In this regard, COFs are not a favorable candidate for photocatalysis of the strong C-F bond cleavage (631.5 KJ/mol) in PFAS, since a small band gap indicates relatively low redox ability [118,119]. However, due to their excellent PFAS adsorption ability [108], high specific surface area, and rapid charge carrier flow, COFs may enhance the performance of other photocatalytic semiconductors, such as titanate oxide (TiO_2), indium oxide (In_2O_3), and gallium oxide (Ga_2O_3), which have proven to be efficient in degrading PFAS [116,118]. The main obstacle to developing hybrid COF-semiconductors is the rigid conditions of their synthesis, which generally requires airtight reactors and non-aqueous organic solvents. Although PFAS degradation using COFs has not yet been reported, endeavors should continue to advance a new generation of hybrid photocatalysts for PFAS defluorination.

5. Factors affecting PFAS removal

It is of practical importance to investigate the influence of the solution chemistry on PFAS removal processes by framework materials. Operating parameters, including solution pH, coexistence of cations/anions, and organic matter, are discussed in regards to their effect on PFAS removal.

5.1. Solution pH

The solution pH can significantly influence the adsorptive removal efficiency of contaminants, since the adsorbent's surface charge and the contaminants' chemical speciation are affected. In general, many PFAS are exist in their anionic form in all relevant environments because their acid dissociation constant (pK_a) values are quite low (from −3.27 to 0.4) [25]. When the adsorbent is present at a pH higher than its point of zero charge (pH_{pzc}), the low degree of protonation makes the surface negatively charged, further increasing the electrostatic interactions with PFAS anions [120].

For instance, Fe-BEA35′s zeta potential becomes more negative with increasing pH values (i.e. −21 mV at pH = 3, −34 mV at pH = 9) [46]. Significant inhibitory effects of increased pH result from the ligand changes within the zeolite since Fe^{3+} complexed with OH^- under these conditions. Conversely, lower pH can reduce the surface charges' density and further weaken the repulsion between PFOA and the zeolite, allowing for adsorption.

Different framework materials have different pH_{pzc} and various interaction mechanisms for adsorbing PFAS. Therefore, the influence of solution pH on PFAS removal should be taken into consideration during removal experiments and carefully investigated to optimize the reaction conditions.

5.2. Inorganic ions

Inorganic ions in the aqueous environment have complicated influences on PFAS removal including surface-charge neutralization, divalent cation bridging, electrical double-layer compression, salting-out and competitive adsorption [121]. The addition of electrolytes compresses the electrical double layer of adsorbents; thus, the ionic concentration impacts the interaction between PFAS and adsorbent. A slight inhibition of PFOA adsorption by Al-based MOFs was detected with increase of NaCl concentration [82]. The negative surface charges of adsorbent can be neutralized by divalent cations such as Ca^{2+}, Cu^{2+} and Mg^{2+}, increasing its zeta potential at the same time. Divalent cations can also construct a bridge to connect PFAS anions and some negatively charged groups. In groundwater, many cations coexist and may improve PFAS adsorption due to their positive charges.

In contrast, anions in solution can compete with anionic PFAS for adsorption site on a material's surface, depending on both the ionic concentrations and species. Clark et al. [79] explored the effect of coexisting SO_4^{2-}, Cl^-, and Cr(VI) on PFOS removal by UiO-66 and found that the presence of Cl^- at 100 mg/L hardly affected PFOS adsorption, but SO_4^{2-} and Cr(VI) exhibited significant inhibition (SO_4^{2-}: 25–100 mg/L, Cr(VI):5–25 mg/L). SO_4^{2-} and Cr(VI) are competitors for the same sites on UiO-66, but Cl^- already existed within the MOF's pores during synthesis. Similar results were obtained when adding different inorganic anions to the Fe-BEA35/PFOA system. SO_4^{2-} was found to greatly decrease the PFOA removal efficiency, which might be attributed to the competitive complexation with Fe^{3+} and quenching effect toward photo-generated hydroxyl radicals ($^{\bullet}OH$) [46]. It is expected that other anions, will also inhibit PFAS adsorption and degradation due to their negative charge.

5.3. Dissolved organic matter (DOM)

The coexistence of DOM possibly disturbs the PFAS removal process. Some researchers noticed that DOM coincides with PFAS in regards to its molecular structure. The highly aromatic structure contributes to hydrophobic regions of the DOM, enabling the hydrophobic interactions between PFAS and DOM [122]. Normally, DOM contains both anionic and cationic group. Thus, electrostatic interactions or cation bridging might occur between the DOM and PFAS. Moreover, DOM can complex with active metal sites and inhibited PFAS adsorption [123]. Regarding photocatalytic degradation, the discovery that DOM can adsorb photoenergy and scavenge photo-activated species suggests inhibition of PFAS degradation [124].

Most studies focused on the adsorptive removal of PFAS by different framework materials are conducted in pure, synthetic solutions. Fulvic (FA) and humic acids (HA) are always chosen to model DOM when evaluating its effect on PFAS removal. However, a variety of organic substrates, such as proteins, amino and carboxylic acids, make up DOM in reality. Thus, some potential interactions between real water matrix and PFAS have not been investigated in detail and further studies of DOM's effects are still needed.

It is noted that these influencing factors were mostly focused on their impacts on PFAS adsorption on framework materials. The matrix effect is also of great practical importance for degradation processes, although the framework material-based defluorination are not well studied yet, even at the laboratory scale. When applying framework materials to remove PFAS from water, these influencing factors need to be examined individually due to the large number of framework materials with different physiochemical properties.

6. Problems and challenges

6.1. Low environmental concentration

In order to estimate the impacts of initial contaminant concentration on the removal kinetics and energy inputs, the concentrations should be set at a reasonable level when testing framework materials for PFAS removal. In the literature, most PFAS removal experiments have been conducted under very high concentrations, up to hundreds of mg/L. Then, the results from adsorption and oxidation batch experiments are used to simulate the potential efficiency of sorbents, although the actual PFAS concentrations in most aquatic environment (except for some AFFF-impacted sites) are extremely low (ng/L to μg/L) [48].

Furthermore, the detection of low PFAS concentrations demands sensitive equipment, including liquid chromatography−tandem mass spectrometry. These advanced instruments are very expensive and difficult to master [125]. Thus, more accessible methods and online measurement of PFAS are needed in both natural and engineered water systems. In some experiments, total organic carbon (TOC) and total fluorine (TF) have been used as proxies for estimating PFAS concentration and defluorination over time; however, this approach still requires knowledge of the initial PFAS concentrations.

6.2. Reactor design

Framework materials are usually in powdered form. Despite their high treatment capacity, the separation and recovery of powders from water presents an engineering challenge. Current efforts primarily focus on immobilizing framework materials on membranes [126,127] or granular particles, such as activated carbon or biochar [128–130]. Both granular adsorbent and membrane treatment units are widely used water treatment technologies, and containment in reactors simplifies their operations. There are many commercially available reactor designs, depending on the particle size. In granular adsorbent reactors, typical media can be easily swapped for modified media. However, these units may require additional, downstream filtration to capture any modified particles leaving the reactor.

On the other hand, for membranes, separation and recovery occur in one reactor. Due to their versatile structures, regular and adjustable pore sizes, various functionalities, and large specific surface area, interest has surged in using framework materials as fillers or coating layers in advanced membrane processes. [131,132] Their intrinsic porosity provides molecular transport pathways that can lower the resistance of internal diffusion and improve water permeability. Additionally, with regular backflushing and chemical cleaning with desorption solvents, researchers have demonstrated that membrane regeneration and cyclical reuse is feasible.

6.3. Stability and reusability

Although the efficacy of framework materials is still under debate, the regeneration of used sorbents is always needed for all removal processes. Discarding framework materials is a serious waste of resources and may cause secondary pollution if the PFAS released to the environment. Regeneration processes often consume harmful chemicals or require a large energy input, yet still the PFAS are merely transfered from the sorbents to another phase. The complete decomposition of PFAS requires powerful destruction means to treat concentrated regeneration solutions [69,133].

Improving the regeneration capability is not only the way to diminish the impact of framework material sorbents to environment, it can also enhance their economic competitiveness with traditional commercialized sorbents (GAC and ion exchange resins) [134]. Research into synthesized framework materials should include appropriate regeneration methods, which preserve their adsorption and catalysis abilities to the greatest extent. Furthermore, the environmental friendliness and cost of regeneration should be evaluated, including proper handling and treatment of eluted wastes.

The structure and functionality of spent sorbents are crucial for the regeneration performance in corresponding desorption process. Typical regeneration methods include washing with (1) an organic solvent (e.g., methanol, ethyl acetate, acetone); (2) an alkaline solution (e.g., NaOH, aqueous ammonia); (3) an acidic solution (e.g., HCl, orthophosphoric); (4) a NaCl solution; or (5) their mixtures [32,82,83]. Chemical solutions made of sodium salt and organic solvents are most commonly used for desorbing PFAS, where the sodium salt separates the anionic head while organic alcohol desorbs the hydrophobic tail [32]. Normally, over 90 % regeneration can be achieved by a solution of sodium hydroxide and methanol [69]. However, the co-adsorbed organic matter on sorbents may decrease regeneration performance, requiring harsher acid/base regeneration solutions. The stability of spent materials must be considered when they are exposed to extremely acid or alkaline conditions.

The composition of the regeneration solution significantly affects the desorption efficiency depending on the different adsorption mechanism. Wang et al. [86] investigated the COFs regeneration after adsorbing GenX and HFPO-TA by using mixture solutions containing salt and organic solvents. GenX can be easily desorbed from the used COFs by 1 % NaCl, but 70 % methanol was not favorable. However, 1 % NaCl can hardly regenerate spent COFs adsorbed HFPO-TA due to their strong affinity; 70 % methanol with the dosage of 1 % NaCl are quite efficient for desorbing HFPO-TA from the spent COFs.

Under some circumstances, an acidic regeneration solution is a viable option. For example, after adsorbing PFBS, the saturated NU-1000 was transferred into a 10 mL regeneration solution consisting of 0.1 M HCl/methanol (30/70 v/v), then undergoes sonication and shaking [135]. After repeating this procedure three times, the treated adsorbent was dried under nitrogen for 0.5 h before use. The NU-1000 exhibited good stability and reusability, with excellent removal and recovery efficiency after five cycles.

6.4. Contamination risks

For any materials or technologies applied in water/wastewater treatment, the potential contamination risks must be carefully assessed before usage. Framework materials are prepared from metal or nonmetal precursors, some of which are not stable in the aquatic environment, especially when the water matrix is complex. Leaching of the metal ions or organic linkers may occur during PFAS removal by framework materials, leading to secondary contamination. The leaching from sorbents and catalysts must be well below the limits set by relevant water treatment standards.

In addition, destructive treatment techniques may create toxic transformation products, subsequently released into the aquatic environment [136]. Research into the degradation mechanisms and pathways is critical to determine potential intermediate compounds. Unfortunately, even when byproducts can be identified, bioaccumulation and toxicology data is often unavailable; therefore, more ecotoxicology research is also required.

7. Conclusions and perspectives

The current review summarized the structure and synthesis of three typical framework materials: zeolites, MOFs, and COFs, and the mechanisms involved in their removal of PFAS. The morphology, crystal structure, pore volume and size, and surface functional groups play dominant roles in the adsorption of PFAS. Among the three framework materials, zeolites often have lower preparation cost and the hydrated aluminosilicates crystals are endowed with high thermal stability and acid resistance, which outperforms most MOFs and COFs. The pore sizes of zeolites usually range from 0.3 to 1 nm and their specific surface area (S_{BET}) are between 600 and 780 m^2/g (Table 2). As for MOFs, various combination of metal species and organic linkers, as well as novel synthesis methods make the structure and property more diverse. A significant difference is that the S_{BET} of different MOFs varies from 12 to 1811 m^2/g. Thanks to the huge specific surface area and tailored surface chemistry, MOFs exhibited best performance in removing both PFOA and PFOS with highest adsorption capacity. Obviously, few researchers have investigated the removal of short-chain PFAS, since they are less adsorbable and more persistent. COFs have been utilized for removing GenX and HFPO-TA and achieved excellent removal efficiency. Some similarities between COFs and MOFs are recognized, including high specific surface area (as high as 1900 m^2/g) [[85]], variable pore structure, and tunable surface functional groups. It is thus important to design and prepare suitable framework materials for remediating specific PFAS in aqueous environment. In particular, PFAS hemi-micelles and micelles can be accommodated by suitable pore sizes of sorbents, preventing the blockage of pores. Surface modifications by adding protonated amine groups can enhance anionic PFAS adsorption via electrostatic attraction. Other interaction mechanisms between framework materials and PFAS include hydrophobic interactions, ligand and ion exchange, hydrogen bonding and π-π interactions. The PFAS molecular structure and the solution chemistry affect the removal performance by framework materials. We also highlighted the challenges in current research efforts, including low environmental concentrations, reactor design, the stability and reusability of framework materials, and contamination risks during water treatment.

The demand for engineering innovations to upgrade existing water facilities and the invention of new technologies and materials is increasing, in order to achieve sustainable PFAS removal and defluorination. Functional framework materials are one promising tool in this regard because their versatile structure and surface chemistry can be tuned to favor PFAS interactions and designed for circular regeneration to minimize or eliminate secondary contamination. Going forward, four guiding principles are proposed for the development of sustainable framework materials to remove PFAS:

Table 2
PFAS adsorption by framework materials.

Framework materials		S_{BET} (m^2/g)	Pore size/ volume	Organic	Sorption capacity	Conditions (P: PFAS, S: sorbent)	Removal rates	Mechanism	Ref.
Zeolite	zeolite 13X	/	1.0 nm	PFOS	/	P=15-150 mg/L (100 mL), S=100 mg, pH=7.2	/	hydrophobic interaction	[59]
	NaY	700	0.8 nm		12		/		
	NaY80	780	0.6 nm		114.7		/		
	all-Si Beta	624	0.21 cm^3/g	PFOA	371.4	P=100 mg/L (5 mL), S=5 mg	/	hydrophobic interaction	[60]
				PFOS	/		/		
	Fe-BEA35	600	0.42 cm^3/g	PFOA	16.8	P=48 uM/L (100 mL), S=100 mg, pH=5.5, UV365+UV254	99 %	electrostatic interactions, hydrophobic interactions	[46]
				PFOS	19.6	P=40 uM/L (350 mL), S=175 mg, pH=5.5, UV254	99 %		[47]
MOFs	MIL-101(Cr)-QDMEN	1530	/	PFOA	753.5	P=40 mL, S=4 mg, pH=5	/	Lewis acid/base complexation, electrostatic interaction	[74]
	ZIF-7	14	/	PFOA	21.5	P=0.5 mM (40 mL), S=8 mg, pH=5	/	/	[75]
	ZIF-8	1291	< 2nm		177.2		/	/	
	ZIF-L	12	/		243.8		/	/	
	SCU-8	1360	2.2 nm	PFOS	44.79	P=1mg/L (40 mL), S=200 mg	/	hydrogen bonds, electrostatic, hydrophobic and van der Waals interactions	[76]
	UiO-66	/	/	PFOA	388	P=500 mg/L, m/V=1	/	hydrophobic and van der Waals interaction	[77]
				PFOS	467		/		
	UiO-66-(F4)	682	/	PFOA	160		/		
				PFOS	254		/		
	Cr-MIL-101	/	2.9-3.4 nm	PFOS	/	P=10 mM (1 mL), S=10 mg	/	/	[78]
	Fe-MIL-101	/			/		/		
	Defective UiO-66	1423	1.6-2 nm 0.72 cm^3/g	PFOS PFBS	620 520.3	P=500 mg/L (200 mL), S=0.5 g/L	/ /	electrostatic and hydrophobic interactions	[79]
	CAT-ZIF-8	1154	1-1.5 nm	PFOA	/	P=20 μM (1 mL), S=20 μL, pH=7	84.5 %	/	[80]
	Fe-BTC	1051	/	PFOA	418	P=500 mg/L (20 mL), S=20 mg, pH=3.3	/	Lewis acid/base complexing and hydrophobic interaction	[81]
	MIL-100-Fe	1237	0.55 nm	PFOA	349		/		
	MIL-101-Fe	1811	1.08, 1.2 nm	PFOA	370		/		
	Basolite A100 MOF	/	/	PFOA	169	P=1 mg/L (40 mL), S=2.5 mg	~70 %	hydrophobic and electrostatic interactions	[82]
	MIL-96-RHPAM2	75	/	PFOA	340	P=1000 mg/L (20 mL), S=20 mg	/	electrostatic and van der Waals interaction, hydrogen bonds	[83]
	MIL-125-NH_2	/	0.82 nm	PFOA	42	P=500 mg/L	/	/	[84]
				PFOS	17		/		
COFs	28%[NH_2]-COF	1900	3 nm, 1.06 cm^3/g	Gen X	200	P=0.2-100 mg/L S=100 mg/L	> 90 %	/	[85]
	BT-BDB-COF (COF2)	28.5	/	Gen X HFPO-TA	679.8 1071.4	P=0.05–0.6 mmol/L (50 mL), pH=7, S=50 mg/L	80 % 100 %	hydrophobic interaction	[86]

1) Environment-friendly and low-cost raw materials are necessary. Although morphology and material properties can be optimized, designers should strive to synthesize the framework materials from sustainable, inexpensive raw materials. The scale-up of the most promising framework materials requires lower economic costs. Theoretical calculation assisted molecular design can be combined with experimental data to develop framework materials with high adsorptive capacity, selectivity, stability, and reusability. A clear regeneration strategy for framework materials is key to compete with commonly used adsorbents.
2) The current state of research on PFAS removal in real water matrices and treatment applications is still nascent and insufficient for industrial adoption. Most studies reported excellent PFAS removal efficiency when pure water or synthetic solution was spiked with high PFAS concentration in a small reaction system. However, the components of real water matrices are far more complicated, especially for those adsorbents relying on hydrophobic interactions to trap PFAS molecules. Future framework material studies should focus on alternative adsorption mechanisms in real water matrices, where PFAS removal is less dependent upon hydrophobic and electrostatic interactions, especially for the short-chain PFAS.
3) Moreover, the list of PFAS chemicals to be studied, including new alternative products, should be extended. The functional framework materials have the advantage of being tailorable for removing different kinds of PFAS endowed with different molecular size and hydrophobicity/hydrophilicity. The pore size, surface area, and functional groups of zeolites, MOF, and COF can be easily manipulated for the removal of a specific PFAS chemical.
4) Finally, proper engineering design is needed to support powdered framework materials, such as immobilization on granular particles or membranes. Reactor design needs to consider potential material release and other contamination risks, including from regeneration and waste streams. Additional efforts are required to design and test engineered solutions for efficient PFAS removal.

Declaration of Competing Interest

The authors declare that they have no known competing financial interests or personal relationships that could have appeared to influence the work reported in this paper.

Data availability

Data will be made available on request.

Acknowledgments

This work was supported by Aarhus University Centre for Water Technology (AU-WATEC) Start-Up Fund from Grundfos Foundation, Aarhus University Research Foundation Starting Grant (No. AUFF-E-

2019-7-28), Novo Nordisk Fonden (No. NNF20OC0064799), Independent Research Fund Denmark Sapere Aude Award (No. 1051-00058B), and China Scholarship Council (No. 201906120393).

Appendix A. Supplementary data

Supplementary data to this article can be found online at https://doi.org/10.1016/j.cej.2022.139202.

References

[1] H. Liang, Y.T. Ying, H. Sun, H.M. Ang, M. Tadé, S. Wang, Solution combustion synthesis of Co oxide-based catalysts for phenol degradation in aqueous solution, J Colloid. Interf. Sci. 372 (2012) 58–62.

[2] R.C. Buck, J. Franklin, U. Berger, J.M. Conder, I.T. Cousins, P. de Voogt, A. A. Jensen, K. Kannan, S.A. Mabury, S.P. van Leeuwen, Perfluoroalkyl and polyfluoroalkyl substances in the environment: Terminology, classification, and origins, Integr. Environ. Asses. 7 (2011) 513–541.

[3] A. Zaggia, L. Conte, L. Falletti, M. Fant, A. Chiorboli, Use of strong anion exchange resins for the removal of perfluoroalkylated substances from contaminated drinking water in batch and continuous pilot plants, Water Res. 91 (2016) 137–146.

[4] R.A. Dickman, D.S. Aga, A review of recent studies on toxicity, sequestration, and degradation of per- and polyfluoroalkyl substances (PFAS), J. Hazard. Mater. 436 (2022), 129120.

[5] Fan, Li, Jun, Duan, Shuting, Tian, Haodong, Ji, Yangmo, Zhu, Short-chain per- and polyfluoroalkyl substances in aquatic systems: Occurrence, impacts and treatment, Chem. Eng. J., 380 (2020) 122506-122506.

[6] S. Kurwadkar, J. Dane, S.R. Kanel, M.N. Nadagouda, R.W. Cawdrey, B. Ambade, G.C. Struckhoff, R. Wilkin, Per- and polyfluoroalkyl substances in water and wastewater: A critical review of their global occurrence and distribution, Sci. Total Environ. 809 (2022), 151003.

[7] K. Prevedouros, I.T. Cousins, R.C. Buck, S.H. Korzeniowski, Sources, Fate and Transport of Perfluorocarboxylates, Environ. Sci. Technol. 40 (2006) 32–44.

[8] Z. Wang, I.T. Cousins, M. Scheringer, R.C. Buck, K. Hungerbühler, Global emission inventories for C4–C14 perfluoroalkyl carboxylic acid (PFCA) homologues from 1951 to 2030, Part I: production and emissions from quantifiable sources, Environ. Int., 70 (2014) 62-75.

[9] K.S. Guruge, L. Yeung, L. Peng, S. Taniyasu, N. Yamashita, M. Nakamura, Fluorinated alkyl compounds including long chain carboxylic acids in wild bird livers from Japan, Chemosphere 83 (2011) 379–384.

[10] S. Rayne, K. Forest, Perfluoroalkyl sulfonic and carboxylic acids: A critical review of physicochemical properties, levels and patterns in waters and wastewaters, and treatment methods, J Environ. Sci. Heal. A. 44 (2009) 1145–1199.

[11] USEPA, Sulfonated Perfluorochemicals in the Environment: Sources, Dispersion, Fate and Effects, https://www.regulations.gov/document/EPA-HQ-OPPT-2002-0043-0005 (accessed April 2022).

[12] J.R. Masoner, D.W. Kolpin, I.M. Cozzarelli, K.L. Smalling, S.C. Bolyard, J.A. Field, E.T. Furlong, J.L. Gray, D. Lozinski, D. Reinhart, A. Rodowa, P.M. Bradley, Landfill leachate contributes per-/poly-fluoroalkyl substances (PFAS) and pharmaceuticals to municipal wastewater, Environ. Sci.: Water Res. & Technol. 6 (2020) 1300–1311.

[13] C. Kunacheva, S. Fujii, S. Tanaka, S.T.M.L.D. Seneviratne, N.P.H. Lien, M. Nozoe, K. Kimura, B.R. Shivakoti, H. Harada, Worldwide surveys of perfluorooctane sulfonate (PFOS) and perfluorooctanoic acid (PFOA) in water environment in recent years, Water Sci. Technol. 66 (2012) 2764–2771.

[14] I.E. Jogsten, G. Perelló, X. Llebaria, E. Bigas, R. Martí-Cid, A. Kärrman, J. L. Domingo, Exposure to perfluorinated compounds in Catalonia, Spain, through consumption of various raw and cooked foodstuffs, including packaged food, Food Chem. Toxicol. 47 (2009) 1577–1583.

[15] V. Mulabagal, L. Liu, J. Qi, C. Wilson, J.S. Hayworth, A rapid UHPLC-MS/MS method for simultaneous quantitation of 23 perfluoroalkyl substances (PFAS) in estuarine water, Talanta 190 (2018) 95–102.

[16] I. Ericson Jogsten, M. Nadal, B. van Bavel, G. Lindström, J.L. Domingo, Per- and polyfluorinated compounds (PFCs) in house dust and indoor air in Catalonia, Spain: Implications for human exposure, Environ. Int. 39 (2012) 172–180.

[17] J.L. Domingo, Health risks of dietary exposure to perfluorinated compounds, Environ. Int. 40 (2012) 187–195.

[18] X. Duan, H. Sun, Y. Wang, J. Kang, S. Wang, N-Doping-Induced Nonradical Reaction on Single-Walled Carbon Nanotubes for Catalytic Phenol Oxidation, ACS Catal. 5 (2015) 553–559.

[19] G.W. Olsen, J.M. Burris, D.J. Ehresman, J.W. Froehlich, A.M. Seacat, J. L. Butenhoff, L.R. Zobel, Half-life of serum elimination of perfluorooctanesulfonate, perfluorohexanesulfonate, and perfluorooctanoate in retired fluorochemical production workers, Environ. Health. Persp. 115 (2007) 1298–1305.

[20] S.E. Fenton, A. Ducatman, A. Boobis, J.C. DeWitt, C. Lau, C. Ng, J.S. Smith, S. M. Roberts, Per- and polyfluoroalkyl substance toxicity and human health review: current state of knowledge and strategies for informing future research, Environ. Toxicol. Chem. 40 (2021) 606–630.

[21] UN environment programme, All pops listed in the Stockholm Convention, http://www.pops.int/TheConvention/ThePOPs/AllPOPs/tabid/2509/Default.aspx.

[22] S. Brendel, É. Fetter, C. Staude, L. Vierke, A. Biegel-Engler, Short-chain perfluoroalkyl acids: Environmental concerns and a regulatory strategy under REACH, Environ. Sci. Eur. 30 (2018) 9.

[23] J. Ao, T. Yuan, H. Xia, Y. Ma, Z. Shen, R. Shi, Y. Tian, J. Zhang, W. Ding, L. Gao, X. Zhao, X. Yu, Characteristic and human exposure risk assessment of per- and polyfluoroalkyl substances: A study based on indoor dust and drinking water in China, Environ. Pollut. 254 (2019), 112873.

[24] Y. Zhou, Z. Zhou, Y. Lian, X. Sun, Y. Wu, L. Qiao, M. Wang, Source, transportation, bioaccumulation, distribution and food risk assessment of perfluorinated alkyl substances in vegetables: A review, Food Chem. 349 (2021), 129137.

[25] E. Steinle-Darling, M. Reinhard, Nanofiltration for trace organic contaminant removal: Structure, solution, and membrane fouling effects on the rejection of perfluorochemicals, Environ. Sci. Technol. 42 (2008) 5292–5297.

[26] J. Yu, J. Hu, S. Tanaka, S. Fujii, Perfluorooctane sulfonate (PFOS) and perfluorooctanoic acid (PFOA) in sewage treatment plants, Water Res. 43 (2009) 2399–2408.

[27] E. Sinclair, K. Kannan, Mass loading and fate of perfluoroalkyl surfactants in wastewater treatment plants, Environ. Sci. Technol. 40 (2006) 1408–1414.

[28] Y. Zhu, H. Ji, K. He, L. Blaney, T. Xu, D. Zhao, Photocatalytic degradation of GenX in water using a new adsorptive photocatalyst, Water Res. 220 (2022), 118650.

[29] J.M. Arana Juve, F. Li, Y. Zhu, W. Liu, L.D.M. Ottosen, D. Zhao, Z. Wei, Concentrate and degrade PFOA with a photo-regenerable composite of In-doped TNTs@AC, Chemosphere 300 (2022), 134495.

[30] Q. Zhou, S. Ma, S. Zhan, Superior photocatalytic disinfection effect of Ag-3D ordered mesoporous CeO_2 under visible light, Appl. Catal. B-Environ. 224 (2018) 27–37.

[31] G. Rothenberg, Catalysis: Concepts and green applications, Adv. Synth. Catal. 350 (2008) 2133–2134.

[32] M. Ateia, A. Alsbaiee, T. Karanfil, W. Dichtel, Efficient PFAS removal by amine-functionalized sorbents: Critical review of the current literature, Environ. Sci. Tech. Let. 6 (2019) 688–695.

[33] D.Q. Zhang, W.L. Zhang, Y.N. Liang, Adsorption of perfluoroalkyl and polyfluoroalkyl substances (PFASs) from aqueous solution - A review, Sci. Total Environ. 694 (2019), 133606.

[34] D. Alezi, Y. Belmabkhout, M. Suyetin, P.M. Bhatt, Ł.J. Weseliński, V. Solovyeva, K. Adil, I. Spanopoulos, P.N. Trikalitis, A.H. Emwas, M. Eddaoudi, MOF crystal chemistry paving the way to gas storage needs: aluminum-based soc-MOF for CH_4, O_2, and CO_2 storage, J. Am. Chem. Soc. 137 (2015) 13308–13318.

[35] K.J. Hartlieb, J.M. Holcroft, P.Z. Moghadam, N.A. Vermeulen, M.M. Algaradah, M.S. Nassar, Y.Y. Botros, R.Q. Snurr, J.F. Stoddart, CD-MOF: A versatile separation medium, J. Am. Chem. Soc. 138 (2016) 2292–2301.

[36] N.A. Khan, Z. Hasan, S.H. Jhung, Adsorptive removal of hazardous materials using metal-organic frameworks (MOFs): A review, J. Hazard. Mater. 244–245 (2013) 444–456.

[37] L. Jiao, Y. Wang, H.L. Jiang, Q. Xu, Metal-Organic Frameworks As Platforms For Catalytic Applications, Adv. Mater. 30 (2018) 1703663.

[38] H.C.J. Zhou, S. Kitagawa, Metal–organic frameworks (MOFs), Chem. Soc. Rev. 43 (2014) 5415–5418.

[39] X. Zhu, H. Zheng, X. Wei, Z. Lin, L. Guo, B. Qiu, G. Chen, Metal–organic framework (MOF): a novel sensing platform for biomolecules, Chem. Commun. 49 (2013) 1276–1278.

[40] B.M. Weckhuysen, J. Yu, Recent advances in zeolite chemistry and catalysis, Chem. Soc. Rev. 44 (2015) 7022–7024.

[41] M. Moshoeshoe, M.S. Nadiye-Tabbiruka, V. Obuseng, A review of the chemistry, structure, properties and applications of zeolites, Am. J. Mater. Sci. 7 (2017) 196–221.

[42] H. Li, M. Eddaoudi, M. O'Keeffe, O.M. Yaghi, Design and synthesis of an exceptionally stable and highly porous metal-organic framework, Nature 402 (1999) 276–279.

[43] O.M. Yaghi, M.J. Kalmutzki, C.S. Diercks, Emergence of metal-organic frameworks, introduction to reticular chemistry, Angew. Chem. Int. Ed. 58 (2019) 1–27.

[44] O.M. Yaghi, M.J. Kalmutzki, C.S. Diercks, Historical perspective on the discovery of covalent organic frameworks, introduction to reticular chemistry, Angew. Chem. Int. Ed. 58 (2019) 177–195.

[45] B.P. Biswal, S. Chandra, S. Kandambeth, B. Lukose, T. Heine, R. Banerjee, Mechanochemical synthesis of chemically stable isoreticular covalent organic frameworks, J. Am. Chem. Soc. 135 (2013) 5328–5331.

[46] L. Qian, A. Georgi, R. Gonzalez-Olmos, F.D. Kopinke, Degradation of perfluorooctanoic acid adsorbed on Fe-zeolites with molecular oxygen as oxidant under UV-A irradiation, Appl. Catal. B-Environ. 278 (2020), 119283.

[47] L. Qian, F.D. Kopinke, A. Georgi, Photodegradation of Perfluorooctanesulfonic Acid on Fe-Zeolites in Water, Environ. Sci. Technol. 55 (2021) 614–622.

[48] S.P. Lenka, M. Kah, L.P. Padhye, A review of the occurrence, transformation, and removal of poly- and perfluoroalkyl substances (PFAS) in wastewater treatment plants, Water Res. 117187 (2021).

[49] E.M. Bell, S. De Guise, J.R. McCutcheon, Y. Lei, M. Levin, B. Li, J.F. Rusling, D. A. Lawrence, J.M. Cavallari, C. O'Connell, B. Javidi, X. Wang, H. Ryu, Exposure, health effects, sensing, and remediation of the emerging PFAS contaminants – Scientific challenges and potential research directions, Sci. Total Environ. 780 (2021), 146399.

[50] D.M. Wanninayake, Comparison of currently available PFAS remediation technologies in water: A review, J. Environ. Manage. 283 (2021), 111977.

[51] Z. Wei, T. Xu, D. Zhao, Treatment of per- and polyfluoroalkyl substances in landfill leachate: status, chemistry and prospects, Environ. Sci. Water Res. Technol. 5 (2019) 1814–1835.

[52] L. Vilà-Nadal, L. Cronin, Design and synthesis of polyoxometalate-framework materials from cluster precursors, Nat. Rev. Mater. 2 (2017) 17054.

[53] J. Weitkamp, Zeolites and catalysis, Solid State Ionics 131 (2000) 175–188.

[54] E.M. Flanigen, A Review and new perspectives in zeolite crystallization, Molecular Sieves, Adv. Chem. 121 (1973) 119–139.

[55] Z. Huang, S. Seo, J. Shin, B. Wang, R.G. Bell, S.B. Hong, X. Zou, 3D–3D topotactic transformation in aluminophosphate molecular sieves and its implication in new zeolite structure generation, Nat. Commun. 11 (2020) 3762.

[56] N. Kosinov, J. Gascon, F. Kapteijn, E.J.M. Hensen, Recent developments in zeolite membranes for gas separation, J. Membr. Sci. 499 (2016) 65–79.

[57] E. Alver, A.Ü. Metin, Anionic dye removal from aqueous solutions using modified zeolite: Adsorption kinetics and isotherm studies, Chem. Eng. J. 200–202 (2012) 59–67.

[58] T. Ennaert, J. Van Aelst, J. Dijkmans, R. De Clercq, W. Schutyser, M. Dusselier, D. Verboekend, B.F. Sels, Potential and challenges of zeolite chemistry in the catalytic conversion of biomass, Chem. Soc. Rev. 45 (2016) 584–611.

[59] M.V.D. Bergh, A. Krajnc, S. Voorspoels, S.R. Tavares, D.E.D. Vos, Highly selective removal of perfluorinated contaminants by adsorption on all-silica zeolite beta, Angew. Chem. 132 (2020).

[60] V. Ochoa, Herrera, R, Sierra, Alvarez, Removal of perfluorinated surfactants by sorption onto granular activated carbon, zeolite and sludge, Chemosphere 72 (2008) 1588–1593.

[61] D. Saliba, M. Ammar, M. Rammal, M. Al-Ghoul, M. Hmadeh, Crystal Growth of ZIF-8, ZIF-67, and Their Mixed-Metal Derivatives, J. Am. Chem. Soc. 140 (2018) 1812–1823.

[62] M. Dusselier, M.E. Davis, Small-Pore Zeolites: Synthesis and Catalysis, Chem. Rev. 118 (2018) 5265–5329.

[63] X. Sun, W. Ji, S. Hou, X. Wang, Facile synthesis of trifluoromethyl covalent organic framework for the efficient microextraction of per-and polyfluorinated alkyl substances from milk products, J. Chromatogr. A 1623 (2020), 461197.

[64] S.H. Jhung, J.H. Lee, J.W. Yoon, C. Serre, G. Férey, J.S. Chang, Microwave synthesis of chromium terephthalate MIL-101 and its benzene sorption ability, Adv. Mater. 19 (2007) 121–124.

[65] W. Ji, Y.S. Guo, H.M. Xie, X. Wang, X. Jiang, D.S. Guo, Rapid microwave synthesis of dioxin-linked covalent organic framework for efficient micro-extraction of perfluorinated alkyl substances from water, J. Hazard. Mater. 397 (2020), 122793.

[66] A. Martinez Joaristi, J. Juan-Alcañiz, P. Serra-Crespo, F. Kapteijn, J. Gascon, Electrochemical synthesis of some archetypical Zn^{2+}, Cu^{2+}, and Al^{3+} metal organic frameworks, Cryst. Growth Des. 12 (2012) 3489–3498.

[67] T. Stolar, L. Batzdorf, S. Lukin, D. Žilić, C. Motillo, T. Friščić, F. Emmerling, I. Halasz, K. Užarević, In situ monitoring of the mechanosynthesis of the archetypal metal–organic framework HKUST-1: Effect of liquid additives on the milling reactivity, Inorg. Chem. 56 (2017) 6599–6608.

[68] D.A. Yang, H.Y. Cho, J. Kim, S.-T. Yang, W.S. Ahn, CO$_2$ capture and conversion using Mg-MOF-74 prepared by a sonochemical method, Energ, Environ. Sci. 5 (2012) 6465–6473.

[69] E. Gagliano, M. Sgroi, P.P. Falciglia, F.G.A. Vagliasindi, P. Roccaro, Removal of poly- and perfluoroalkyl substances (PFAS) from water by adsorption: Role of PFAS chain length, effect of organic matter and challenges in adsorbent regeneration, Water Res. 171 (2020), 115381.

[70] S. Adam, A. Ellern, K. Seppelt, Structural principles of the coordination number eight: WF, ReF, and XeF, Chem. Eur. J. 2 (1996) 398–402.

[71] J.R. Li, H.C. Zhou, Metal–organic hendecahedra assembled from dinuclear paddlewheel nodes and mixtures of ditopic linkers with 120 and 90° bend angles, Angew. Chem. Int. Ed. 48 (2009) 8465–8468.

[72] J.R. Li, H.C. Zhou, Bridging-ligand-substitution strategy for the preparation of metal–organic polyhedra, Nat. Chem. 2 (2010) 893–898.

[73] H.C. Zhou, J.R. Long, O.M. Yaghi, Introduction to metal-organic frameworks, Chem. Rev. 112 (2012) 673–674.

[74] K. Liu, S. Zhang, X. Hu, K. Zhang, A. Roy, G. Yu, Understanding the adsorption of PFOA on MIL-101(Cr)-based anionic-exchange metal–organic frameworks: comparing DFT calculations with aqueous sorption experiments, Environ. Sci. Technol. 49 (2015) 8657–8665.

[75] M.J. Chen, A.C. Yang, N.H. Wang, H.C. Chiu, Y.L. Li, D.Y. Kang, S.L. Lo, Influence of crystal topology and interior surface functionality of metal-organic frameworks on PFOA sorption performance, Micropor. Mesopor. Mat. 236 (2016) 202–210.

[76] Y. Li, Z. Yang, Y. Wang, Z. Bai, T. Zheng, X. Dai, S. Liu, D. Gui, W. Liu, M. Chen, L. Chen, J. Diwu, L. Zhu, R. Zhou, Z. Chai, T.E. Albrecht-Schmitt, S. Wang, A mesoporous cationic thorium-organic framework that rapidly traps anionic persistent organic pollutants, Nat. Commun. 8 (2017) 1354.

[77] K. Sini, D. Bourgeois, M. Idouhar, M. Carboni, D. Meyer, Metal–organic framework sorbents for the removal of perfluorinated compounds in an aqueous environment, New J. Chem. 42 (2018) 17889–17894.

[78] D. Barpaga, J. Zheng, K.S. Han, J.A. Soltis, V. Shutthanandan, S. Basuray, B. P. McGrail, S. Chatterjee, R.K. Motkuri, Probing the sorption of perfluorooctanesulfonate using mesoporous metal–organic frameworks from aqueous solutions, Inorg. Chem. 58 (2019) 8339–8346.

[79] C.A. Clark, K.N. Heck, C.D. Powell, M.S. Wong, Highly defective UiO-66 materials for the adsorptive removal of perfluorooctanesulfonate, ACS Sustain. Chem. Eng. 7 (2019) 6619–6628.

[80] Z. Guo, J. Liu, Y. Li, J.A. McDonald, M.Y. Bin Zulkifli, S.J. Khan, L. Xie, Z. Gu, B. Kong, K. Liang, Biocatalytic metal–organic framework nanomotors for active water decontamination, Chem. Commun. 56 (2020) 14837–14840.

[81] Y. Yang, Z. Zheng, W. Ji, J. Xu, X. Zhang, Insights to perfluorooctanoic acid adsorption micro-mechanism over Fe-based metal organic frameworks: Combining computational calculation with response surface methodology, J Hazar. Mater. 395 (2020), 122686.

[82] B.M. Jun, H.S. Hwang, J. Heo, J. Han, M. Jang, J. Sohn, C.M. Park, Y. Yoon, Removal of selected endocrine-disrupting compounds using Al-based metal organic framework: Performance and mechanism of competitive adsorption, J. Ind. Eng. Chem. 79 (2019) 345–352.

[83] L.H. Mohd Azmi, D.R. Williams, B.P. Ladewig, Polymer-assisted modification of metal-organic framework MIL-96 (Al): influence of HPAM concentration on particle size, crystal morphology and removal of harmful environmental pollutant PFOA, Chemosphere 262 (2021), 128072.

[84] O.K. Ozdemir, J.M. Ornstein, A novel, nanostructured, metal-organic frameworks-based pretreatment technology for the remediation of PFAS in industrial wastewater, TechConnect, Briefs (2019).

[85] W. Ji, L. Xiao, Y. Ling, C. Ching, M. Matsumoto, R.P. Bisbey, D.E. Helbling, W. R. Dichtel, Removal of GenX and perfluorinated alkyl substances from water by amine-functionalized covalent organic frameworks, J. Am. Chem. Soc. 140 (2018) 12677–12681.

[86] W. Wang, Z. Zhou, H. Shao, S. Zhou, G. Yu, S. Deng, Cationic covalent organic framework for efficient removal of PFOA substitutes from aqueous solution, Chem. Eng. J. 412 (2021), 127509.

[87] S. Wuttke, Introduction to Reticular Chemistry. Metal–Organic Frameworks and Covalent Organic Frameworks By Omar M. Yaghi, Markus J. Kalmutzki, and Christian S. Diercks, Angew. Chem. Int. Ed., 58 (2019) 14024-14024.

[88] M. Eddaoudi, J. Kim, N. Rosi, D. Vodak, J. Wachter, M. O'Keeffe, O.M. Yaghi, Systematic design of pore size and functionality in isoreticular mofs and their application in methane storage, Science 295 (2002) 469–472.

[89] S.S.Y. Chui, S.M.F. Lo, J.P.H. Charmant, A.G. Orpen, I.D. Williams, A Chemically functionalizable nanoporous material [Cu$_3$(TMA)$_2$(H$_2$O)$_3$]$_n$, Science 283 (1999) 1148–1150.

[90] O.K. Farha, C.E. Wilmer, I. Eryazici, B.G. Hauser, P.A. Parilla, K. O'Neill, A. A. Sarjeant, S.T. Nguyen, R.Q. Snurr, J.T. Hupp, Designing higher surface area metal–organic frameworks: are triple bonds better than phenyls? J. Am. Chem. Soc. 134 (2012) 9860–9863.

[91] O.K. Farha, A.M. Shultz, A.A. Sarjeant, S.T. Nguyen, J.T. Hupp, Active-site-accessible, porphyrinic metal−organic framework materials, J. Am. Chem. Soc. 133 (2011) 5652–5655.

[92] Z. Guo, H. Wu, G. Srinivas, Y. Zhou, S. Xiang, Z. Chen, Y. Yang, W. Zhou, M. O'Keeffe, B. Chen, A metal–organic framework with optimized open metal sites and pore spaces for high methane storage at room temperature, Angew. Chem. Int. Ed. 50 (2011) 3178–3181.

[93] H. Hayashi, A.P. Côté, H. Furukawa, M. O'Keeffe, O.M. Yaghi, Zeolite A imidazolate frameworks, Nat. Mater. 6 (2007) 501–506.

[94] D.Y. Hong, Y.K. Hwang, C. Serre, G. Férey, J.S. Chang, porous chromium terephthalate mil-101 with coordinatively unsaturated sites: Surface functionalization, encapsulation, sorption and catalysis, Adv. Funct. Mater. 19 (2009) 1537–1552.

[95] C. Zhao, Y. Xu, F. Xiao, J. Ma, Y. Zou, W. Tang, Perfluorooctane sulfonate removal by metal-organic frameworks (MOFs): Insights into the effect and mechanism of metal nodes and organic ligands, Chem. Eng. J. 406 (2021), 126852.

[96] J.C. Moreton, J.M. Palomba, S.M. Cohen, Liquid-Phase Applications of Metal–organic framework mixed-matrix membranes prepared from poly (ethylene-co-vinyl acetate), ACS Appl. Polym. Mater. 2 (2020) 2063–2069.

[97] Y. Pi, X. Li, Q. Xia, J. Wu, Y. Li, J. Xiao, Z. Li, Adsorptive and photocatalytic removal of Persistent Organic Pollutants (POPs) in water by metal-organic frameworks (MOFs), Chem. Eng. J. 337 (2018) 351–371.

[98] Q. Wang, J. Lu, Y. Jiang, S. Yang, Y. Yang, Z. Wang, FeCo bimetallic metal organic framework nanosheets as peroxymonosulfate activator for selective oxidation of organic pollutants, Chem. Eng. J. 443 (2022), 136483.

[99] M. Pu, Z. Guan, Y. Ma, J. Wan, Y. Wang, M.L. Brusseau, H. Chi, Synthesis of iron-based metal-organic framework MIL-53 as an efficient catalyst to activate persulfate for the degradation of Orange G in aqueous solution, Appl. Catal. A-Gen. 549 (2018) 82–92.

[100] T.W. Goh, C. Xiao, R.V. Maligal-Ganesh, X. Li, W. Huang, Utilizing mixed-linker zirconium based metal-organic frameworks to enhance the visible light photocatalytic oxidation of alcohol, Chem. Eng. Sci. 124 (2015) 45–51.

[101] C.C. Wang, X.H. Yi, P. Wang, Powerful combination of MOFs and C$_3$N$_4$ for enhanced photocatalytic performance, Appl. Catal. B-Enviro. 247 (2019) 24–48.

[102] L. Shen, S. Liang, W. Wu, R. Liang, L. Wu, CdS-decorated UiO–66(NH$_2$) nanocomposites fabricated by a facile photodeposition process: An efficient and stable visible-light-driven photocatalyst for selective oxidation of alcohols, J. Mater. Chem. A 1 (2013) 11473–11482.

[103] S. Kandambeth, K. Dey, R. Banerjee, Covalent Organic Frameworks: Chemistry beyond the Structure, J. Am. Chem. Soc. 141 (2019) 1807–1822.

[104] D. Cui, Y. Fang, O. MacLean, D.F. Perepichka, F. Rosei, S. Clair, Covalent organic frameworks from a monomer with reduced symmetry: polymorphism and Sierpiński triangles, Chem. Commun. 55 (2019) 13586–13589.

[105] D. Beaudoin, T. Maris, J.D. Wuest, Constructing monocrystalline covalent organic networks by polymerization, Nat. Chem. 5 (2013) 830–834.

[106] F.J. Uribe-Romo, J.R. Hunt, H. Furukawa, C. Klöck, M. O'keeffe, O.M. Yaghi, A crystalline imine-linked 3-D porous covalent organic framework, J. Am. Chem. Soc., 131 (2009) 4570-4571.

[107] C.R. DeBlase, W.R. Dichtel, moving beyond boron: The emergence of new linkage chemistries in covalent organic frameworks, Macromolecules 49 (2016) 5297–5305.

[108] X. Chen, W.D. Oh, T.T. Lim, Graphene- and CNTs-based carbocatalysts in persulfates activation: Material design and catalytic mechanisms, Chem. Eng. J. 354 (2018) 941–976.

[109] M. Di, L. Hu, L. Gao, X. Yan, W. Zheng, Y. Dai, X. Jiang, X. Wu, G. He, Covalent organic framework (COF) constructed proton permselective membranes for acid supporting redox flow batteries, Chem. Eng. J. 399 (2020), 125833.

[110] L. Deng, X. Kang, K. Zhang, M. Gao, Q. Fu, Z. Xia, D. Gao, Fabrication of covalent organic frameworks and its selective extraction of fluoronitrobenzenes from environmental samples, J. Chromatogr. A 1635 (2021), 461704.

[111] Y.J. Hou, J. Deng, K. He, C. Chen, Y. Yang, Covalent organic frameworks-based solid-phase microextraction probe for rapid and ultrasensitive analysis of trace per- and polyfluoroalkyl substances using mass spectrometry, Anal. Chem. 92 (2020) 10213–10217.

[112] P. Pachfule, A. Acharjya, J. Roeser, T. Langenhahn, M. Schwarze, R. Schomäcker, A. Thomas, J. Schmidt, diacetylene functionalized covalent organic framework (cof) for photocatalytic hydrogen generation, J. Am. Chem. Soc. 140 (2018) 1423–1427.

[113] X. Wang, L. Chen, S.Y. Chong, M.A. Little, Y. Wu, W.H. Zhu, R. Clowes, Y. Yan, M. A. Zwijnenburg, R.S. Sprick, A.I. Cooper, Sulfone-containing covalent organic frameworks for photocatalytic hydrogen evolution from water, Nat. Chem. 10 (2018) 1180–1189.

[114] S. Lin, C.S. Diercks, Y.B. Zhang, N. Kornienko, E.M. Nichols, Y. Zhao, A.R. Paris, D. Kim, P. Yang, O.M. Yaghi, C.J. Chang, Covalent organic frameworks comprising cobalt porphyrins for catalytic CO_2 reduction in water, Science 349 (2015) 1208.

[115] H. Lv, X. Zhao, H. Niu, S. He, Z. Tang, F. Wu, J.P. Giesy, Ball milling synthesis of covalent organic framework as a highly active photocatalyst for degradation of organic contaminants, J. Hazard. Mater. 369 (2019) 494–502.

[116] Q. Yang, M. Luo, K. Liu, H. Cao, H. Yan, Covalent organic frameworks for photocatalytic applications, Appl. Catal. B-Environ. 276 (2020), 119174.

[117] T. Sick, A.G. Hufnagel, J. Kampmann, I. Kondofersky, M. Calik, J.M. Rotter, A. Evans, M. Döblinger, S. Herbert, K. Peters, D. Böhm, P. Knochel, D.D. Medina, D. Fattakhova-Rohlfing, T. Bein, Oriented films of conjugated 2D covalent organic frameworks as photocathodes for water splitting, J. Am. Chem. Soc. 140 (2018) 2085–2092.

[118] B. Xu, M.B. Ahmed, J.L. Zhou, A. Altaee, M. Wu, G. Xu, Photocatalytic removal of perfluoroalkyl substances from water and wastewater: Mechanism, kinetics and controlling factors, Chemosphere 189 (2017) 717–729.

[119] J. Wang, C. Cao, Y. Zhang, Y. Zhang, L. Zhu, Underneath mechanisms into the super effective degradation of PFOA by BiOF nanosheets with tunable oxygen vacancies on exposed (101) facets, Appl. Catal. B-Environ. 286 (2021), 119911.

[120] C.T. Vu, T. Wu, Recent progress in adsorptive removal of per- and poly-fluoroalkyl substances (PFAS) from water/wastewater, Crit. Rev. Environ. Sci. Technol. 1–40 (2020).

[121] Z. Du, S. Deng, Y. Bei, Q. Huang, B. Wang, J. Huang, G. Yu, Adsorption behavior and mechanism of perfluorinated compounds on various adsorbents—A review, J. Hazard. Mater. 274 (2014) 443–454.

[122] D.N. Kothawala, S.J. Köhler, A. Östlund, K. Wiberg, L. Ahrens, Influence of dissolved organic matter concentration and composition on the removal efficiency of perfluoroalkyl substances (PFASs) during drinking water treatment, Water Res. 121 (2017) 320–328.

[123] C. Mikutta, R. Kretzschmar, Spectroscopic evidence for ternary complex formation between arsenate and ferric iron complexes of humic substances, Environ. Sci. Technol. 45 (2011) 9550–9557.

[124] X. Liang, J. Cheng, C. Yang, S. Yang, Factors influencing aqueous perfluorooctanoic acid (PFOA) photodecomposition by VUV irradiation in the presence of ferric ions, Chem. Eng. J. 298 (2016) 291–299.

[125] L. Ahrens, Polyfluoroalkyl compounds in the aquatic environment: A review of their occurrence and fate, J. Environ. Monitor. 13 (2011) 20–31.

[126] S.F. Seyedpour, A. Rahimpour, G. Najafpour, Facile in-situ assembly of silver-based MOFs to surface functionalization of TFC membrane: A novel approach toward long-lasting biofouling mitigation, J. Membr. Sci. 573 (2019) 257–269.

[127] X.Y. Gong, Z.H. Huang, H. Zhang, W.L. Liu, X.H. Ma, Z.L. Xu, C.Y. Tang, Novel high-flux positively charged composite membrane incorporating titanium-based MOFs for heavy metal removal, Chem. Eng. J. 398 (2020), 125706.

[128] C.A.F. de Oliveira, F.F. da Silva, G.C. Jimenez, J.F. da S. Neto, D.M.B. de Souza, I. A. de Souza, S.A. Júnior, MOF@activated carbon: A new material for adsorption of aldicarb in biological systems, Chem. Commun., 49 (2013) 6486-6488.

[129] A.M. Aldawsari, I.H. Alsohaimi, H.M.A. Hassan, M.R. Berber, Z.E.A. Abdalla, I. Hassan, E.A.M. Saleh, B.H. Hameed, Activated carbon/MOFs composite: AC/NH_2-MIL-101(Cr), synthesis and application in high performance adsorption of p-nitrophenol, J. Saudi Chem. Soc. 24 (2020) 693–703.

[130] F.N. Azad, M. Ghaedi, K. Dashtian, S. Hajati, V. Pezeshkpour, Ultrasonically assisted hydrothermal synthesis of activated carbon–HKUST-1-MOF hybrid for efficient simultaneous ultrasound-assisted removal of ternary organic dyes and antibacterial investigation: Taguchi optimization, Ultrason. Sonochem. 31 (2016) 383–393.

[131] X. Cheng, X. Jiang, Y. Zhang, C.H. Lau, Z. Xie, D. Ng, S.J.D. Smith, M.R. Hill, L. Shao, Building additional passageways in polyamide membranes with hydrostable metal organic frameworks to recycle and remove organic solutes from various solvents, ACS Appl. Mater. Interf. 9 (2017) 38877–38886.

[132] H. Fan, J. Gu, H. Meng, A. Knebel, J. Caro, High-flux membranes based on the covalent organic framework COF-LZU1 for selective dye separation by nanofiltration, Angew. Chem. Int. Ed. 57 (2018) 4083–4087.

[133] P.J. Huang, M. Hwangbo, Z. Chen, Y. Liu, J. Kameoka, K.H. Chu, Reusable functionalized hydrogel sorbents for removing long- and short-chain perfluoroalkyl acids (PFAAs) and GenX from aqueous solution, ACS Omega 3 (2018) 17447–17455.

[134] D. Lu, S. Sha, J. Luo, Z. Huang, X. Zhang Jackie, Treatment train approaches for the remediation of per- and polyfluoroalkyl substances (PFAS): A critical review, J. Hazard. Mater., 386 (2020) 121963.

[135] R. Li, S. Alomari, R. Stanton, M.C. Wasson, T. Islamoglu, O.K. Farha, T.M. Holsen, S.M. Thagard, D.J. Trivedi, M. Wriedt, Efficient removal of per- and polyfluoroalkyl substances from water with zirconium-based metal–organic frameworks, Chem. Mater. 33 (2021) 3276–3285.

[136] J. Cui, P. Gao, Y. Deng, Destruction of per- and polyfluoroalkyl substances (PFAs) with advanced reduction processes (ARPs): A critical review, Environ. Sci. Technol. 54 (2020) 3752–3766.